

1 **Enhancement of snow albedo reduction and radiative forcing**
2 **due to coated black carbon in snow**

3 Wei Pu¹, Tenglong Shi¹, Jiecan Cui¹, Yang Chen¹, Yue Zhou¹, Xin Wang^{1,2}

4

5 ¹Key Laboratory for Semi-Arid Climate Change of the Ministry of Education, College
6 of Atmospheric Sciences, Lanzhou University, Lanzhou 730000, China

7 ²Institute of Surface-Earth System Science, Tianjin University, Tianjin 300072, China

8

9 Corresponding author: Xin Wang (wxin@lzu.edu.cn)

10

11

12

1 **Abstract.** When black carbon (BC) is internally mixed with other atmospheric particles,
2 BC light absorption is effectively enhanced. This study explicitly resolved the optical
3 properties of coated BC in snow, based on core/shell Mie theory and a snow, ice, and
4 aerosol radiative model (SNICAR). Our results indicate that a ‘BC coating effect’
5 enhances the reduction of snow albedo by a factor of 1.1–1.8 for a non-absorbing shell
6 and 1.1–1.3 for an absorbing shell, depending on BC concentration, snow grain radius,
7 and core/shell ratio. We develop parameterizations of the BC coating effect for
8 application to climate models, which provides a convenient way to accurately estimate
9 the climate impact of BC in snow. Finally, based on a comprehensive set of in situ
10 measurements across the Northern Hemisphere, we find that the contribution of the BC
11 coating effect to snow light absorption has exceeded that of dust over northern China.
12 Notably, the high enhancements of snow albedo reductions by BC coating effect were
13 found in the Arctic and Tibetan Plateau, suggesting a greater contribution of BC to the
14 retreat of Arctic sea ice and Tibetan glaciers.
15

1 **1 Introduction**

2 Snow is the most reflective natural substance at Earth's surface and covers more
3 than 30% of global land area (Cohen and Rind, 1991). Snow albedo feedback is
4 considered one of the major energy balance factors of the climate system. Previous
5 observations have revealed that light-absorbing particles (LAPs; e.g., black carbon
6 (BC), organic carbon (OC), and mineral dust) within snow can reduce snow albedo and
7 enhance the absorption of solar radiation (Hadley and Kirchstetter, 2012). As a result,
8 LAPs play a significant role in altering snow morphology and snowmelt processes, and
9 therefore have important effects on local hydrological cycles and global climate (Qian
10 et al., 2009).

11 Given the importance of the climate feedback caused by LAPs in snow, studies
12 have developed snow radiative models and sought to improve our understanding of the
13 influence of LAP-contaminated snow on climate. For example, Warren and Wiscombe
14 (1980) developed a radiative forcing model based on Mie theory and δ -Eddington
15 approximation, and reported that snow albedo in visible wavelengths could be reduced
16 by 5%–15% when 1000 ng g^{-1} BC is present in snow. Flanner et al. (2007) developed
17 a more comprehensive snow albedo model (the snow, ice, and aerosol radiation model;
18 SNICAR) for multilayer snowpack using the two-stream radiative transfer solution. In
19 addition to BC, the SNICAR model also accounts for the potential effects of dust
20 particles and volcanic ash on snow albedo. Recently, some studies indicated that the
21 mixing state of BC and snow could effectively change snow albedo (Liou et al., 2011,

1 2014; Flanner et al., 2012; Liu et al., 2012; He et al., 2017, 2018a, b, c). Moreover,
2 snow grain shape also has an important influence on snow albedo (Kokhanovsky and
3 Zege, 2004). Nonspherical snow grains have weaker albedo reduction than snow
4 spheres (He et al., 2018c; Dang et al., 2016).

5 Although efforts have been made to optimize snow albedo models, current models
6 still suffer from major limitations. Studies have indicated that when BC in the
7 atmosphere is coated with other aerosols it can significantly enhance light absorption
8 via a lensing effect compared with uncoated BC, as investigated using model
9 simulations (e.g., Jacobson 2001; Matsui et al., 2018) and experimental measurements
10 (e.g., Cappa et al., 2012; Peng et al., 2016). Moreover, coated BC has been observed to
11 exist for only a few hours after emission in some regions (Moteki et al., 2007; Moffet
12 and Prather, 2009). Global aerosol models that simulate microphysical processes have
13 indicated that most BC is mixed with other particles within 1–5 days (Jacobson, 2001)
14 at all altitudes (Aquila et al., 2011). However, a problem is that whether coated BC is
15 existed in real snowpack because the coating materials (e.g. salts and OC) of coated BC
16 may be dissolved during wet deposition. A recent study observing individual particle
17 structure and mixing states between the glacier–snowpack and atmosphere based on
18 field measurements and laboratory transmission electron microscope (TEM) and
19 energy dispersive X-ray spectrometer (EDX) instrument analysis (Dong et al., 2018)
20 told the truth. They found that the salt-coated BC was still observed in real snowpack
21 in spite of its lower proportion than that in the atmosphere due to the dissolution effect

1 within precipitating snow. For OC, that study didn't observe reduced OC components
2 in LAPs. More notably, that study further found that the proportion of coated BC was
3 even higher in snowpack than that in the atmosphere. All of the above observation
4 results demonstrated that the coated BC particles are existed in real snowpack and even
5 more common than that in the atmosphere. Hence, the climate impacts of BC must be
6 evaluated in the context of the effect of coating on light absorption enhancement.

7 Although the BC coating effect on light absorption enhancement in the atmosphere
8 is broadly acknowledged, little research has been carried out on snow albedo. Flanner
9 et al. (2007) developed the first radiative transfer model to investigate the coating effect
10 on snow albedo, using sulfate as the BC particle coating with a constant absorption
11 enhancement factor of ~ 1.5 . Subsequently, Wang et al. (2017) used a similar constant
12 light absorption enhancement factor for their spectral albedo model for dirty snow
13 (SAMDS). However, the factor varies with the optical properties of different coatings,
14 the core/shell ratio, wavelength, and other parameters in real environments (Lack and
15 Cappa, 2010; Liu et al., 2017). For example, Liu et al. (2017) reported that the core/shell
16 ratio is a key control on light absorption enhancement. You et al. (2016) suggested that
17 light absorption enhancement is highly correlated with visible or near-infrared (NIR)
18 wavelengths and coating material. Furthermore, a core/shell Mie theory simulation
19 (Lack and Cappa, 2010) found light absorption enhancement was smaller for mildly
20 absorbing coatings (e.g., OC) than non-absorbing coatings (e.g., sulfate). Hence, using
21 a constant enhancement factor will result in biased simulation estimates, against

1 refining our knowledge of the hydrological and climate impacts of BC in snow.

2 In this study we apply core/shell Mie theory to calculate the optical properties of
3 BC coated with both mildly absorbing OC and non-absorbing sulfate, and use these
4 results within a SNICAR model to evaluate the influence on snow albedo.
5 Parameterizations for the BC coating effect are then developed for application in other
6 snow albedo and climate models. Finally, we estimate the enhancements of snow albedo
7 reductions and associated radiative forcing by the BC coating effect across the Northern
8 Hemisphere, by combining model simulations with in situ observations of BC and OC
9 concentrations in snow.

10 **2 Methods**

11 **2.1 Modeling**

12 **2.1.1 Optical parameter calculations for coated BC**

13 Figure 1a and 1c shows schematics of light absorption by externally and internally
14 mixed particles (EMP and IMP, respectively). EMP refers to uncoated BC mixed with
15 other particles, while IMP refers to BC that is assumed to be a core coated by another
16 particle acting as a shell (Kahnert et al., 2012). For a non-absorbing shell, overall light
17 absorption includes contributions from the BC core and enhancement absorption from
18 a lensing effect, while for an absorbing shell, the shell itself also contributes to light
19 absorption. The lensing effect means that when BC is coated with the non-absorbing
20 shell (or the absorbing shell), the shell acts as a lens and focuses more photons onto the
21 core than would reach it otherwise, so that the light absorption by the BC core can be

1 enhanced (Bond et al., 2006).

2 To evaluate the BC coating effect on snow albedo, it is necessary to determine the
3 optical parameters of coated BC. The refractive index (RI) of BC was assumed to be
4 $1.95-0.79i$ following Lack and Cappa (2010), which is consistent with the original
5 SNICAR model (Flanner et al., 2007). Two types of particle shells (non-absorbing and
6 absorbing) were considered. The non-absorbing shell was represented using sulfate,
7 and its RI was assumed to be $1.55-10^{-6}i$ following the atmospheric study of Bond et al.
8 (2006). The absorbing shell was represented using OC, which is a major light-absorbing
9 particle in snow (Wang et al., 2013). The RI of OC varies with wavelength. Here, a
10 fixed mass absorption coefficient (MAC) for OC of $0.3 \text{ m}^2 \text{ g}^{-1}$ at 550 nm, a real RI of
11 1.55, and a particle diameter of 200 nm were assumed, following the observations of
12 Yang et al. (2009) and the study of Lack and Cappa (2010). The uncertainty of snow
13 albedo of coated BC due to OC MAC will be discussed in Section 3.4. Based on Mie
14 theory, an imaginary RI value of $-1.36 \cdot 10^{-2}i$ at 550 nm was calculated. Subsequently,
15 wavelength-dependent imaginary RI values (Figure S1) were derived according to an
16 absorption angstrom exponent (AAE) of -6 (Sun et al., 2007).

17 For a core/shell-structured particle, the core and shell diameters refer to the BC
18 core diameter and the whole particle diameter, respectively. BC diameters are usually
19 in the range of $\sim 50-120$ nm in the atmosphere (Corbin et al., 2018), and are typically
20 larger by ~ 20 nm in snow due to a removal process via wet deposition (Schwarz et al.,
21 2013). Therefore, we assumed the BC diameter in snow was 100 nm with a fixed

1 monodisperse size distribution. The uncertainty of snow albedo of coated BC due to
2 BC size distribution will be discussed in Section 3.4. The shell diameter was assumed
3 from 110 nm to 300 nm based on Bond et al. (2006). Core and shell diameters, RI, and
4 wavelength were then used in a Mie model to derive optical parameters of the core/shell
5 particle, including single scatter albedo (SSA), asymmetry factor (g), and extinction
6 cross-section (Q_{ext}). The mass extinction coefficient (MEC) of the core/shell particle
7 was calculated based on Q_{ext} and the density, given as 1.8 g cm^{-3} for BC (Bond et al.,
8 2006), 1.2 g cm^{-3} for sulfate, and 1.2 g cm^{-3} for OC (Turpin and Lim, 2001).

9 **2.1.2 Snow albedo calculations**

10 We simulated snow albedo with the SNICAR model (Flanner et al., 2007), which
11 calculates the radiative transfer in snowpack based on the theory of Warren and
12 Wiscombe (1980) and a two-stream multilayer radiative approximation (Toon et al.,
13 1989). Here, we summarize only the model features in SNICAR that are crucial to our
14 study. SNICAR allows for a vertical multilayer distribution of snow properties, LAPs,
15 and heating throughout the snowpack column. Input optical parameters (MEC, SSA,
16 and g) of snow grains and BC were calculated off-line using Mie theory. SNICAR
17 provides albedo changes from uncoated and sulfate-coated BC on snow, as well as dust
18 particles and volcanic ash (for further details, see Flanner et al., 2007).

19 In this study, we assumed a homogeneous semi-infinite snowpack and a solar
20 zenith angle of 49.5° , whose cosine value (0.65) represents the insolation-weighted
21 mean solar zenith cosine for sunlit Earth hemisphere (Dang et al., 2015). The snow

1 grain optical effective radius varied from 50 to 1000 μm (with a 50- μm interval) to
2 characterize snow aging. Meanwhile, BC concentrations were assumed in the range of
3 0-1000 ng g^{-1} (with a 10- ng g^{-1} interval) to demonstrate clear to polluted snow, which
4 was based on the global field observations with BC concentrations in snowpack mostly
5 below 1000 ng g^{-1} (e.g. Doherty et al., 2010, 2014; Wang et al., 2013; Li et al., 2017,
6 2018; Pu et al., 2017; Zhang et al., 2017, 2018). These parameters are also applied for
7 parameterizations (see Section 2.3). In addition, we note the SNICAR used in this study
8 was default version that assumes BC-snow external mixing and snow spheres (Flanner
9 et al., 2007). Although the mixing state of BC and snow grains, and snow grain shape
10 can affect the snow albedo, the empirical parameterizations for the effect of BC
11 internally mixed with snow grains on snow albedo has been developed by He et al.
12 (2018c), and the albedo of a snowpack consisting of nonspherical snow grains can be
13 mimicked by using a smaller grain of spherical shape (Dang et al. 2016). Therefore,
14 users can combine the empirical parameterizations by He et al. (2018c) and Dang et al.
15 (2016) with the empirical parameterizations by us (see Section 2.3) to study the effect
16 of the internal mixing of BC with snow grains, snow grain shape, and coated BC on
17 snow albedo.

18 For SNICAR snow albedo simulations of uncoated BC, concentrations of both BC
19 and other particles were input directly. For coated BC, optical parameters (MEC, SSA,
20 and g) of IMP (calculated above) were first archived as lookup tables within SNICAR,
21 and then the concentration of IMP was input.

1 2.2 Calculation of broadband snow albedo

2 The spectral albedo (α_λ) was integrated over the solar spectrum ($\lambda = 300\text{--}2500\text{ nm}$)
3 and weighted by the incoming solar irradiance (S_λ) to calculate broadband snow albedo
4 ($\alpha_{\text{integrated}}$):

$$5 \quad \alpha_{\text{integrated}} = \frac{\int \alpha_\lambda S_\lambda d_\lambda}{\int S_\lambda d_\lambda} \quad (1)$$

6 The incoming solar irradiance was a typical surface solar spectrum for mid–high
7 latitudes from January to May, calculated with the Santa Barbara DISORT Atmospheric
8 Radiative Transfer (SBDART) model (Pu et al., 2019), which is one of the most widely
9 used models for radiative transfer simulations (for further details, see Ricchiuzzi et al.
10 1998).

11 2.3 Parameterizations

12 In the original SNICAR model, the BC coating effect is simply parameterized with
13 an absorption enhancement of ~ 1.5 (Flanner et al., 2007). However, the effect of BC
14 coating on snow albedo is widely variable and dependent on BC concentration,
15 core/shell ratio, snow grain size, and the type of particle shell (see Section 3.3). In view
16 of this complexity, more explicit parameterizations were developed in this study:

$$17 \quad E_{\alpha, \text{integrated}} = \frac{\alpha_{\text{int, integrated}}}{\alpha_{\text{ext, integrated}}} \quad (2)$$

18 where $\alpha_{\text{ext, integrated}}$ and $\alpha_{\text{int, integrated}}$ are broadband snow albedos for EMP and
19 IMP, respectively. Following a previous empirical formulation (Hadley and Kirchstetter,
20 2012), $E_{\alpha, \text{integrated}}$ was parameterized as

$$E_{\alpha,\text{integrated,para}} = a_0 \times (C_{BC})^{a_1} + a_2 \quad (3)$$

$$a_1 = b_0 \times (\log_{10}(R_{\square f}/50))^{b_1} \quad (4)$$

where $E_{\alpha,\text{integrated,para}}$ is the parameterized $E_{\alpha,\text{integrated}}$, C_{BC} is the BC concentration, and $R_{\square f}$ represents the snow grain radius. The terms a_0 , a_1 , a_2 , b_0 , and b_1 are the empirical coefficients and dependent on the core/shell ratio and the type of particle shell. To enhance the precision, parameterizations were divided into two groups: the first to account for relatively clean snow (with BC concentrations $< 200 \text{ ng g}^{-1}$) and the second for relatively polluted snow ($200 \text{ ng g}^{-1} < \text{BC concentrations} < 1000 \text{ ng g}^{-1}$).

2.4 Calculation of in situ snow albedo and radiative forcing

In situ broadband clear-sky ($\alpha_{\text{integrated}}^{\text{clear,in-situ}}$) and cloudy-sky ($\alpha_{\text{integrated}}^{\text{cloudy,in-situ}}$) albedos were calculated separately based on in situ snow-LAP parameters and SBDART simulated clear-sky and cloudy-sky incoming solar irradiance. We assumed a semi-infinite snowpack due to limited snow depth measurements. BC and OC concentrations were collected from in situ field measurements (e.g. Doherty et al., 2010, 2014; Wang et al., 2013; Li et al., 2017, 2018; Pu et al., 2017; Zhang et al., 2017, 2018). The snow grain radius of 100 (1000) μm was assumed for fresh (old) snow, which is comparable to previous observations at mid to high latitudes in winter (Wang et al., 2017; Shi et al., 2020). The value of solar zenith angle was calculated based on the longitude, latitude, and sampling time at each sampling site. The in situ all-sky albedo ($\alpha_{\text{integrated}}^{\text{all-sky,in-situ}}$) was then calculated using weighted clear-sky and cloudy-sky albedos depending on cloud

1 fraction (CF), given as:

$$2 \quad \alpha_{\text{integrated}}^{\text{all-sky,in-situ}} = \text{CF} \times \alpha_{\text{integrated}}^{\text{cloudy,in-situ}} + (1 - \text{CF}) \times \alpha_{\text{integrated}}^{\text{clear,in-situ}} \quad (5)$$

3 In situ radiative forcing by LAPs was calculated by multiplying the derived
4 broadband albedo reduction by the downward shortwave flux at the snow surface (Dang
5 et al., 2017). We point out that the radiative forcing was calculated using the January-
6 February average solar radiation for NA and NC, while April-May average solar
7 radiation for the Arctic and TP according to the periods of filed campaigns. In this study,
8 we mainly estimate the relative impact of internal mixing to external mixing on snow
9 albedo and radiative forcing, which is hence not influenced by the chosen solar
10 radiation. Figure S2 shows the spatial distributions of solar flux and cloud fraction,
11 which were obtained from the Clouds and the Earth's Radiant Energy System (CERES)
12 (<https://ceres.larc.nasa.gov/products.php?product=SYN1deg>).

13 **3 Results and discussion**

14 **3.1 Impact on particle light absorption**

15 Figure 1b and 1d shows the light absorption enhancement, E_{abs} for coated BC. E_{abs}
16 is defined as the ratio of the light absorption for coated (LA_{int}) versus uncoated BC
17 (LA_{ext}), ($E_{\text{abs}} = \frac{LA_{\text{int}}}{LA_{\text{ext}}}$). Based on Bond et al. (2006), we show the most common
18 core/shell ratios (the ratio of the diameter of the whole particle to the BC core) of 1.2,
19 1.5, 2.0, and 2.5 in real environments to represent the thickness of shells, and we used
20 detailed core/shell ratios from 1.1 to 3.0 (in intervals of 0.1) for parameterizations (see
21 Section 3.5). E_{abs} varies with the wavelength and increases with core/shell ratio, in

1 contrast to the default E_{abs} value used in the original SNICAR model, which remains
2 constant. For a non-absorbing shell, the light absorption of IMP is larger than EMP
3 across all wavelengths (300–1400 nm). For an absorbing shell, E_{abs} is similar to the
4 non-absorbing shell in NIR, but becomes smaller in visible (VIS) light and ultra-violet
5 (UV), which implies the absorbing shell reduces whole-particle light absorption and
6 contributes negatively to E_{abs} . This is because compared with non-absorbing shell, the
7 absorbing shell although absorbs additional incident photons, but causes fewer to reach
8 the core, so that the photons absorbed by the lensing effect and the BC core will be
9 reduced. In such a case, the additional photons absorbed by the shell are fewer than the
10 reduced number of photons absorbed by the lensing effect and the BC core, causing
11 that the total absorption by absorbing shell coated BC will be smaller than non-
12 absorbing shell coated BC (Lack and Cappa, 2010[石1]). Furthermore, the absorbing
13 shell reduces E_{abs} to <1 in UV at high core/shell ratios, implying that the lensing effect
14 absorption at those wavelengths cannot recover the BC core absorption reduction,
15 resulting in fewer photons reaching the core, which is similar to the results by Lack and
16 Cappa (2010).

17 **3.2 Impact on spectral snow single-scattering properties and albedos**

18 In real snowpack, BC can effectively enhance snow single-scattering co-albedo
19 $(1-\omega)$, but its effect on other snow optical parameters, such as the asymmetry factor
20 and extinction efficiency, is negligible (He et al., 2017). Therefore, we focus our
21 discussion on coating-induced enhancement of snow single-scattering co-albedo ($E_{1-\omega}$),

1 snow albedo (E_α), and snow albedo reduction ($E_{\Delta\alpha}$). The $E_{1-\omega}$ is defined as the ratio of
2 snow single-scattering co-albedo with coated BC ($1-\omega_{\text{int}}$) versus that with uncoated BC
3 ($1-\omega_{\text{ext}}$), ($E_{1-\omega} = \frac{1-\omega_{\text{int}}}{1-\omega_{\text{ext}}}$). Similar definitions were used for E_α ($E_\alpha = \frac{\alpha_{\text{int}}}{\alpha_{\text{ext}}}$) and $E_{\Delta\alpha}$
4 ($E_{\Delta\alpha} = \frac{\Delta\alpha_{\text{int}}}{\Delta\alpha_{\text{ext}}}$), where α_{int} and α_{ext} are snow albedos with coated and uncoated BC,
5 and $\Delta\alpha_{\text{int}}$ and $\Delta\alpha_{\text{ext}}$ are snow albedo reductions due to coated and uncoated BC.

6 Figure 2 shows the varied $1-\omega$ and $E_{1-\omega}$ depending on different BC concentrations,
7 core/shell ratios, and coating materials. For either non-absorbing shell or absorbing
8 shell, $1-\omega_{\text{int}}$ is usually larger than $1-\omega_{\text{ext}}$ in VIS, while the coating effect has little
9 impacts at wavelength > 1200 nm, which is due to that the optical properties of snow
10 is effectively affected by LAPs in VIS, but primarily by snow itself at wavelength $>$
11 1200 nm. In addition, $E_{1-\omega}$ increases with increased core/shell ratios, and the
12 wavelength of maximum $E_{1-\omega}$ value is dependent on BC concentrations and core/shell
13 ratios. Moreover, absorbing shell shows a negative impact for $E_{1-\omega}$ compared with non-
14 absorbing shell, especially in UV.

15 Snow albedo is effectively affected by various factors, such as snow grain size,
16 LAP content, solar zenith angle, which has been widely discussed and verified through
17 model simulation and experimental measurements by previous studies (e.g. Warren and
18 Wiscombe, 1980; Hadley and Kirchstetter, 2012; Wang et al., 2017). In this study, we
19 mainly focus on the coating effect of BC on snow albedo. Figure 3 shows the spectral
20 snow albedos for coated (α_{int}) and uncoated BC (α_{ext}), and the ratios (E_α) of α_{int}
21 versus α_{ext} . In consistent with $1-\omega$, the impact of coating effect on snow albedo mainly

1 presents at wavelength $< \sim 1200$ nm (Figures 3a versus 3b, 3d versus 3e), where the
2 higher the BC concentration is (or the larger the core/shell ratio is), the larger the
3 difference of snow albedos between uncoated and coated BC is. Hadley and Kirchstetter
4 (2012) also found a smaller snow albedo for internal mixed particles relative to that for
5 external mixed particles. This phenomenon is also obvious on E_α , which decreases with
6 increased BC concentration and core/shell ratios in VIS and NIR (Figure 3c and 3f).
7 For a given BC concentration and core/shell ratio, E_α generally decreases with the
8 wavelength from UV to VIS, then increases from VIS to NIR, which is corresponding
9 to the results of E_{abs} and $E_{1-\omega}$. On the other hand, the E_α for non-absorbing and absorbing
10 shell is comparable with each other at wavelength $> \sim 800$ nm. However, when
11 wavelength $< \sim 800$ nm, E_α for absorbing shell is larger than that for non-absorbing shell
12 and the difference increases with the decreased wavelength and increased core/shell
13 ratio. Moreover, for absorbing shell, the snow albedo for coated BC is higher than that
14 for uncoated BC at $< \sim 350$ nm at large core/shell ratios, which are due to that the light
15 absorption by internal mixed particles for absorbing shell is smaller than that by
16 external mixed particles at those wavelengths as discussed in Section 3.1. These results
17 indicate that the material of particle shell also plays an important role for snow albedo
18 in UV and VIS. We note that the solar radiative flux is very small at wavelengths < 350
19 nm, so that the coating effect at those wavelengths may have little contributions to total
20 light absorption and broadband snow albedos, but which may potentially influence the
21 photochemical reactions in snowpack (Grannas et al., 2007).

1 Furthermore, Figure 4 shows the spectral snow albedo reductions caused by coated
 2 ($\Delta\alpha_{\text{int}}$) and uncoated BC ($\Delta\alpha_{\text{ext}}$), and the ratios ($E_{\Delta\alpha}$) of $\Delta\alpha_{\text{int}}$ versus $\Delta\alpha_{\text{ext}}$.
 3 Generally, $\Delta\alpha_{\text{int}}$ is larger than $\Delta\alpha_{\text{ext}}$, and core/shell ratio dominates the variations of
 4 $E_{\Delta\alpha}$ across the wavelengths of 300-1400 nm, while the impact of BC content mainly
 5 focuses on 500-1000 nm. In consistent with $E_{1-\omega}$ and E_a , the impact of the material of
 6 particle shell is negligible at wavelength $> \sim 800$ nm, but the $E_{\Delta\alpha}$ for absorbing shell is
 7 smaller than that for non-absorbing shell at wavelength $< \sim 800$ nm. Moreover, the $E_{\Delta\alpha}$
 8 is < 1 for absorbing shell at wavelength $< \sim 350$ nm at large core/shell ratios. It is
 9 interesting that the coating effect still has an obvious impact on snow albedo reduction
 10 at wavelength $> \sim 1200$ nm, which is different with $E_{1-\omega}$ and E_a .

11 **3.3 Impact on broadband snow single-scattering properties and albedos**

12 Compared with spectral optical properties, our broadband results have wider
 13 implications for the research community. Figure 5 shows the spectrally weighted $1-\omega$
 14 for coated ($1-\omega_{\text{int, integrated}}$) and uncoated BC ($1-\omega_{\text{ext, integrated}}$), and the ratios ($E_{1-\omega, \text{ integrated}}$)
 15 of $1-\omega_{\text{int, integrated}}$ versus $1-\omega_{\text{ext, integrated}}$. In general, $1-\omega_{\text{int, integrated}}$ is larger than $1-\omega_{\text{ext, integrated}}$,
 16 and $E_{1-\omega, \text{ integrated}}$ increased with BC concentration and core/shell ratio, but is
 17 little affected by snow grain size. $E_{1-\omega, \text{ integrated}}$ is in a range of 1.0 to ~ 1.35 and 1.0 to
 18 ~ 1.23 for non-absorbing and absorbing shell, respectively, with BC concentrations
 19 within 1000 ng g^{-1} and core/shell ratios of 1.2-2.5. For a given BC concentration and
 20 core/shell ratio, $E_{1-\omega, \text{ integrated}}$ for non-absorbing shell is larger than that for absorbing
 21 shell. In addition, $E_{1-\omega, \text{ integrated}}$ of the original SNICAR model is closed to that of non-

1 absorbing shell at a core/shell ratio of 1.5.

2 Figure 6 shows the spectrally weighted snow albedo for coated ($\alpha_{\text{int, integrated}}$) and
3 uncoated BC ($\alpha_{\text{ext, integrated}}$), and the ratios ($E_{\alpha, \text{ integrated}}$) of $\alpha_{\text{int, integrated}}$ versus $\alpha_{\text{ext, integrated}}$.
4 Generally, $\alpha_{\text{int, integrated}}$ is smaller than $\alpha_{\text{ext, integrated}}$ by 0 to 0.069 (0 to 0.051), and $E_{\alpha, \text{ integrated}}$
5 $E_{\alpha, \text{ integrated}}$ varies from 1 to ~ 0.903 (1 to ~ 0.924) for non-absorbing (absorbing) shell with
6 BC concentrations from 0 to 1000 ng g⁻¹, snow grain radius from 100 μm to 500 μm ,
7 and core/shell ratios from 1.2 to 2.5. $E_{\alpha, \text{ integrated}}$ shows a decreased trend with increased
8 BC concentration, core/shell ratio and snow grain size. In addition, the difference
9 between $\alpha_{\text{ext, integrated}}$ and $\alpha_{\text{int, integrated}}$ (or $E_{\alpha, \text{ integrated}}$) for non-absorbing shell is larger (or
10 smaller) than that for absorbing shell. If considering these coating effects in real
11 environments. For example, in clean snow, such as North American with a typical BC
12 concentration of ~ 50 ng g⁻¹ (Doherty et al., 2014), the difference between $\alpha_{\text{ext, integrated}}$
13 and $\alpha_{\text{int, integrated}}$ is in a range of 0.002-0.017 and 0.001-0.012 for non-absorbing and
14 absorbing shell, respectively, with core/shell ratios of 1.2-2.5 and snow grain radius of
15 100-500 μm . In contrast, in polluted snow, such as Northeastern China, BC
16 concentration is typically ~ 1000 ng g⁻¹ in industrial regions. the difference between $\alpha_{\text{ext, integrated}}$
17 $\alpha_{\text{ext, integrated}}$ and $\alpha_{\text{int, integrated}}$ ranges from 0.008-0.069 and 0.007-0.051 for non-absorbing and
18 absorbing shell, respectively. The results show that the impact of coating effect on snow
19 albedo can leads the snow albedo reduced by $\sim 2\%$ in clean snow and $\sim 10\%$ in polluted
20 snow for coated BC than that for uncoated BC. In addition, the sensitivity of $E_{\alpha, \text{ integrated}}$
21 to BC decreases with increasing BC concentration due to the nonlinear effect of BC on

1 snow albedo (Flanner et al., 2007).

2 Figure 7 shows the spectrally weighted snow albedo reductions by coated ($\Delta\alpha_{\text{int, integrated}}$) and uncoated BC ($\Delta\alpha_{\text{ext, integrated}}$), and the ratios ($E_{\Delta\alpha, \text{integrated}}$) of $\Delta\alpha_{\text{int, integrated}}$ versus $\Delta\alpha_{\text{ext, integrated}}$. Different from $E_{\alpha, \text{integrated}}$, $E_{\Delta\alpha, \text{integrated}}$ is dominated by core/shell ratio, but little dependent on snow grain size (Figures 7c and 6f). In addition, $E_{\Delta\alpha, \text{integrated}}$ presents a slight decreased trend with increased BC concentration. Comparing Figure 7c and f, we find that the material of particle shell presents a distinct impact on $E_{\Delta\alpha, \text{integrated}}$. $E_{\Delta\alpha, \text{integrated}}$ mostly falls in a range of 1.11 to ~ 1.80 (1.10 to ~ 1.33) for non-absorbing (absorbing) shell with core/shell ratios from 1.2 to 2.5. Our results were comparable with the previous study that the snow albedo reduction of BC-snow internal mixing is larger than external mixing by a factor of 0.2-1.0 (He et al., 2018c). On the other hand, the $E_{\Delta\alpha, \text{integrated}}$ from the original SNICAR model only shows a small variation of 1.23–1.31. This is similar to a non-absorbing shell with a core/shell ratio of ~ 1.5 , which implies the original SNICAR model only reflects a coating effect on snow albedo reduction at an intermediate core/shell ratio and may lead to possible biases of -10% to 50% in snow albedo reduction calculation.

17 **3.4 Uncertainties**

18 Although the imaginary RI value of OC has been theoretically calculated (Section 19 2.1), we note that in real snowpack there is large uncertainty because the types and 20 optical properties of OC varies spatially and temporally due to different emission 21 sources and photochemical reactions in the atmosphere (e.g. Lack and Cappa, 2010).

1 To address this issue, we tested the degree of influence of imaginary RI on $E_{\alpha, \text{integrated}}$,
2 and $E_{\Delta\alpha, \text{integrated}}$ values by increasing and decreasing the calculated imaginary RI by 50%
3 (Figure S1), which studies have shown to be plausible (e.g., Lack et al., 2012). We find
4 imaginary RI uncertainty to be $\pm 1\%$ for $E_{\alpha, \text{integrated}}$ and $\pm 5\%$ for $E_{\Delta\alpha, \text{integrated}}$.

5 In addition, observations show large variation in the size distribution of
6 atmospheric and snow BC particles (Schwarz et al., 2013), which can affect snow
7 optical properties and albedo (He et al., 2018). Therefore, we examined the effects of
8 BC particle size on $E_{\alpha, \text{integrated}}$ and $E_{\Delta\alpha, \text{integrated}}$ with two additional BC diameters of 50
9 nm and 150 nm, which are within observed size ranges (Schwarz et al., 2013) and are
10 comparable to BC particle sizes used in other studies (e.g. He et al., 2018b). We find
11 the uncertainty attributed to BC diameter is $\pm 1\%$ for $E_{\alpha, \text{integrated}}$ and $\pm 13\%$ for $E_{\Delta\alpha, \text{integrated}}$.
12 According to Equation 2, the uncertainty for $E_{\alpha, \text{integrated}}$ is equivalent to that for
13 snow albedo and the uncertainty for $E_{\Delta\alpha, \text{integrated}}$ is equivalent to that for snow albedo
14 reduction. Therefore, the total uncertainty related to imaginary RI and BC diameter is
15 $\pm 1.4\%$ for $E_{\alpha, \text{integrated}}$ (snow albedo) and $\pm 13.9\%$ for $E_{\Delta\alpha, \text{integrated}}$ (snow albedo reduction).

16 Another important issue is that in real environments, BC mixtures with other
17 species are likely much more complex than uniform coatings on spheres, hence a core-
18 shell assumption seems somewhat dubious. However, a recent study observing
19 individual particle structure and mixing states between the glacier–snowpack and
20 atmosphere (Dong et al., 2018) found that fresh BC particles are generally characterized
21 with fractal morphology, which has a large quantity in the atmosphere. In contrast, in

1 the snowpack, aged BC particles dominated the BC content and the mixing states of
2 aged BC particles change largely to the internal mixing forms with BC as the core. This
3 process is characterized by the initial transformation from a fractal structure to spherical
4 morphology and the subsequent growth of fully compact particles during the transport
5 and deposition process. Therefore, a core-shell assumption for coated BC in snowpack
6 seems to be plausible. In addition, most field measurements can not capture the explicit
7 structure of coated BC due to limited observation methods (e.g. Doherty et al., 2010,
8 2014; Wang et al., 2013; Li et al., 2017, 2018; Pu et al., 2017; Zhang et al., 2017, 2018),
9 therefore even if a model for explicit BC structure was developed, researchers are hard
10 to use it for studying the effect of coated BC on snow albedo reductions at present.
11 Moreover, a core-shell assumption for coated BC in the atmosphere has been widely
12 applied by most global climate models (e.g. Jacobson, 2001; Bond et al. 2013), so that
13 our parameterizations for coated BC in snowpack can be easily linked to them. In
14 summary, we indicate that a core-shell assumption for coated BC in snowpack is
15 plausible and practical for field observations and model simulations at present in despite
16 of the possible uncertainties. However, with the developments of measurement methods
17 and climate models, building a more explicit structure for coated BC in snowpack is
18 actually needed in the future.

19 **3.5 Parameterizations of the coating effect**

20 Figure 8 compares parameterized $E_{\alpha, \text{integrated, para}}$ with SNICAR-modeled $E_{\alpha, \text{integrated}}$,
21 and Tables S1 and S2 list the empirical coefficients (see Section 2.3) derived from

1 nonlinear regression processes. This parameterization is under the assumptions of semi-
2 infinite snowpack, BC-snow external mixing, and spherical snow grains as mentioned
3 in Section 2. Generally, $E_{\alpha, \text{integrated, para}}$ and $E_{\alpha, \text{integrated}}$ show a strong correlation, with
4 $R^2 = 0.988$ (0.986) for a non-absorbing shell and $R^2 = 0.987$ (0.986) for an absorbing
5 shell in relatively clean (polluted) snow, and root mean squared errors of $1.81 \cdot 10^{-3}$
6 ($4.70 \cdot 10^{-3}$) and $1.41 \cdot 10^{-3}$ ($3.76 \cdot 10^{-3}$), respectively. Biases for $E_{\alpha, \text{integrated, para}}$ are
7 smallest for intermediate BC concentrations, but become relatively larger at extremely
8 low or high values, due mainly to processes within the nonlinear regression method. In
9 addition, the snow grain size has small impacts on the accuracy of parameterized results,
10 so that the parameterizations can be applied in either fresh snow or old snow types.
11 Overall, the $E_{\alpha, \text{integrated}}$ can be well reproduced by $E_{\alpha, \text{integrated, para}}$ and the
12 parameterizations are applicable in various snow pollution conditions with BC
13 concentrations from 0-1000 ng g^{-1} , core/shell ratios from 1.1 to 3.0, and different
14 coating materials (non-absorbing and absorbing shell). We note that if BC concentration
15 is larger than 1000 ng g^{-1} , the parameterization for relatively polluted snow is also
16 applicable with a small negative bias.

17 Therefore, other studies can estimate the coating effect of BC on snow albedos
18 and radiative forcing very conveniently by combining the original SNICAR or other
19 snow radiative forcing model with our new parameterizations, which may reduce snow
20 albedo simulation bias. On the other hand, although most global climate models (GCMs)
21 account for coated BC in the atmosphere, they barely consider the coating effect for BC

1 in snow (Bond et al., 2013). In addition, different GCMs apply different types of snow
2 radiative transfer models, which means that one physical mechanism responsible for
3 the BC coating effect in snow cannot be suitable for all GCMs. Hence, our
4 parameterizations are good for the climate models to have an option for BC coating
5 effects in snow.

6 **3.6 Measurement-based estimate of coating effect**

7 To evaluate the coating effect of BC on both snow albedo and radiative forcing in
8 real snowpack, we collected in situ measurements of BC and OC concentrations in
9 snow (Figure 9) during field campaigns in the Arctic in spring 2007–2009 (Doherty et
10 al., 2010), North America in January–March 2013 (Doherty et al., 2014), northern
11 China in January–February 2010 and 2012 (Ye et al., 2012; Wang et al., 2013), and the
12 Tibetan Plateau in spring 2010 and 2012 (Wang et al., 2013; Li et al., 2017, 2018; Pu
13 et al., 2017; Zhang et al., 2017, 2018). Measurements are separated into four
14 geographical regions (Figure 9c): the Arctic, North America (NA), northern China
15 (NC), and the Tibetan Plateau (TP). An absorbing shell of OC was assumed in measured
16 snowpack, which is plausible because previous studies have found that OC is the
17 dominant coating in the atmosphere (e.g., Cappa et al., 2012) and snow (Dong et al.,
18 2018). The OC/BC mass ratio is generally from 1 to 10, with the corresponding
19 core/shell ratio from 1.3 to 2.5 (Figure 9b). The average core/shell ratio was highest
20 (2.45) in the TP, followed by 1.92 and 1.81 in the Arctic and NC, respectively, and
21 lowest (1.31) in NA (Figure 9d). These results reveal the BC coating effect had a larger

1 impact on snow albedo in the TP than in other regions. In this study, the assumption
2 that all measured OC resides as coating on BC particles were mainly used to show the
3 upper bound of coating effect on snow albedo reduction, which is comparable with the
4 previous studies (e.g. He et al. 2018c).

5 Figure 10 shows the statistics for snow albedo reductions and radiative forcing in
6 different regions for fresh snow (snow grain radius =100 μm) and old snow (snow grain
7 radius =1000 μm). The spatial distributions of snow albedo reductions and radiative
8 forcing are presented in Figure S3 and S4. Briefly, the TP snowpack suffers the highest
9 snow albedo reduction (0.066), and the regional average snow albedo reductions are
10 lower in NC (0.055), NA (0.009), and the Arctic (0.007) for fresh snow in the case of
11 external mixing (Figure 10a). Accordingly, the regional average radiative forcing is
12 11.63, 4.42, 0.97, and 0.56 W m^{-2} in TP, NC, NA, and the Arctic (Figure 10b). In the
13 case of internal mixing, the regional average snow albedo reductions are 0.084, 0.065,
14 0.011, and 0.009 in TP, NC, NA, and the Arctic, with the corresponding radiative
15 forcing of 14.84, 5.51, 1.11, and 0.69 W m^{-2} . Figure 11 shows the comparisons of
16 internal mixing to external mixing. For fresh snow, we find that coated BC results in
17 greater snow albedo reductions compared with uncoated BC by factors of 1.27, 1.19,
18 1.13, and 1.23 in the TP, NC, NA, and the Arctic, respectively (Figures 11a and 11b).
19 Correspondingly, we find that the coating effect leads radiative forcing by 1.27, 1.20,
20 1.14, and 1.22 for these same regions. The highest (lowest) enhancement was found in
21 the TP (NA), which corresponds to the highest (lowest) OC/BC mass ratio and

1 core/shell ratio in the TP (NA). For old snow, the regional average snow albedo
2 reductions are 0.17 (0.21), 0.14 (0.17), 0.028 (0.033) and 0.022 (0.027) in TP, NC, NA,
3 and the Arctic for external (internal) mixing (Figure 10c). The corresponding radiative
4 forcing are 38.2 (47.6), 19.2 (22.7), 4.6 (5.2) and 3.6 (4.6) W m^{-2} (Figure 10d). The
5 enhancement of snow albedo reductions due to the BC coating effect are 1.24, 1.15,
6 1.13, and 1.23 in TP, NC, NA, and the Arctic, respectively (Figure 11c). The
7 corresponding radiative forcing reductions are 1.24, 1.16, 1.14, and 1.22 (Figure 11d).
8 The enhancement shows a slight decrease with snowpack aging, which is consistent
9 with the results in Figure 7. Of note, we found the contribution of coating effect to light
10 absorption has exceeded dust over most areas of northern China after comparing with
11 previous studies of dust in snow (Wang et al., 2013, 2017; Pu et al., 2017), which further
12 demonstrated the critical role of BC coatings in snow albedo evaluation.

13 In contrast to previous studies, we note that enhanced light absorption in snow
14 from the BC coating effect should be taken into account, especially in the Arctic and
15 the TP. Arctic sea ice has shown a sharp decline in recent decades (Ding et al., 2019),
16 and climate models predict a continued decreasing trend (Liu et al., 2020) that is likely
17 to perturb the Earth system and influence human activities (Meier et al., 2014). Multi-
18 model ensemble simulations indicate that greenhouse gases cannot fully explain this
19 decline, and recent studies have proposed that BC deposition in snow and sea ice is an
20 important additional contributor (e.g., Ramanathan and Carmichael, 2008).
21 Furthermore, the TP holds the largest ice mass outside polar regions, and acts as a water

1 'storage tower' for more than 1 billion people in South and East Asia. Tibetan glaciers
2 have rapidly retreated over the last 30 years (Yao et al., 2012), raising the possibility
3 that many glaciers and their fresh water supplies could disappear by the middle of the
4 21st century. Observed evidence suggests that BC deposition is a significant
5 contributing factor to this retreat (Xu et al., 2009), but quantitatively modeling the effect
6 of BC on glacier dynamics is a challenge, partly because of incomplete radiative
7 transfer mechanisms within models. Due to the significant contribution of BC to
8 retreating Arctic sea ice and Tibetan glaciers, and the strong enhancement of light
9 absorption by coated BC, the coating effect must now be considered in climate models
10 that are designed to accurately reconstruct both the historical record and future change.

11 **4 Conclusions**

12 This study evaluated the effect of BC coating on snow albedo and radiative forcing
13 by combining core/shell Mie theory and the snow-albedo model SNICAR. We found that
14 the coating effect enhances snow albedo reduction by a factor of 1.11–1.80 for a non-
15 absorbing shell and 1.10–1.33 for an absorbing shell, when BC concentrations are
16 within 1000 ng g^{-1} , the snow grain radius is 100–500 μm , and the core/shell ratio is
17 1.2–2.5. The core/shell ratio plays a dominant role in reducing snow albedo.
18 Furthermore, an absorbing shell causes a smaller snow albedo reduction than a non-
19 absorbing shell because of a lensing effect, whereby the absorbing shell reduces photon
20 absorbance in the BC core. Our results can effectively account for the complex
21 enhancement of snow albedo reduction due to coating effect in real environments.

1 Parameterizations for the coating effect are further developed for use in snow
2 albedo and climate models. Parameterized and simulated results show strong
3 correlations for both clean and polluted snowpack. The root mean squared error of
4 parameterized $E_{\alpha, \text{integrated, para}}$ is low ($1.41 \cdot 10^{-3}$). A list of empirical coefficients for
5 parameterizations is provided for most seasonal snowpack field cases, with BC
6 concentrations within 1000 ng g^{-1} , snow grain sizes from 50–1000 μm , and core/shell
7 ratios from 1.1 to 3.0. We demonstrate that parameterizations can reduce simulation
8 bias for local experiments in snow albedo models and, more importantly, can be applied
9 to GCMs to improve our understanding of how BC in snow affects local hydrological
10 cycles and global climate.

11 Based on a comprehensive set of field measurements across the Northern
12 Hemisphere, the BC coating effect in real snowpack was evaluated by assuming the
13 presence of an absorbing OC shell. The enhancement of snow albedo reduction was
14 1.13–1.27 and enhancement of radiative forcing was 1.14–1.27, which exceeds the
15 contribution of dust to snow light absorption over most areas of northern China. Of
16 note, the greatest enhancements were detected on the Tibetan Plateau and in the Arctic,
17 which will likely contribute to further Arctic sea ice and Tibetan glacier retreat. Our
18 findings indicate that the coating effect must be considered in future climate models, in
19 particular to more accurately evaluate the climate of the Tibetan Plateau and the Arctic.

1 **Conflict of interest**

2 The authors declare that they have no conflict of interest.

3 **Acknowledgments**

4 This research was supported jointly by the National Science Fund for
5 Distinguished Young Scholars (42025102), the National Key R&D Program of China
6 (2019YFA0606801), the National Natural Science Foundation of China (42075061,
7 41975157 and 41775144), and the China Postdoctoral Science Foundation
8 (2020M673530).

9 **Author contributions**

10 X Wang and W Pu invited the project. W Pu and X Wang designed the study. W
11 Pu wrote the paper with contributions from all co-authors. TL Shi processed and
12 analyzed the data.

1 **References**

- 2 Aquila, V., Hendricks, J., Lauer, A., Riemer, N., Vogel, H., Baumgardner, D., Minikin,
3 A., Petzold, A., Schwarz, J., and Spackman, J.: MADE-in: A new aerosol
4 microphysics submodel for global simulation of insoluble particles and their
5 mixing state, *Geosci. Model Dev.*, 4, 325-355, 2011.
- 6 Bond, T. C., Habib, G., and Bergstrom, R. W.: Limitations in the enhancement of
7 visible light absorption due to mixing state, *J. Geophys. Res.-Atmos.*, 111, D20,
8 2006.
- 9 Bond, T. C., Doherty, S. J., Fahey, D. W., Forster, P. M., Berntsen, T., DeAngelo, B.
10 J., Flanner, M. G., Ghan, S., Karcher, B., Koch, D., Kinne, S., Kondo, Y., Quinn,
11 P. K., Sarofim, M. C., Schultz, M. G., Schulz, M., Venkataraman, C., Zhang, H.,
12 Zhang, S., Bellouin, N., Guttikunda, S. K., Hopke, P. K., Jacobson, M. Z., Kaiser,
13 J. W., Klimont, Z., Lohmann, U., Schwarz, J. P., Shindell, D., Storelvmo, T.,
14 Warren, S. G., and Zender, C. S.: Bounding the role of black carbon in the climate
15 system: A scientific assessment, *J. Geophys. Res.-Atmos.*, 118, 5380-5552, 2013.
- 16 Cappa, C. D., Onasch, T. B., Massoli, P., Worsnop, D. R., Bates, T. S., Cross, E. S.,
17 Davidovits, P., Hakala, J., Hayden, K. L., Jobson, B. T., Kolesar, K. R., Lack, D.
18 A., Lerner, B. M., Li, S. M., Mellon, D., Nuaaman, I., Olfert, J. S., Petaja, T.,
19 Quinn, P. K., Song, C., Subramanian, R., Williams, E. J., and Zaveri, R. A.:
20 Radiative Absorption Enhancements Due to the Mixing State of Atmospheric
21 Black Carbon, *Science*, 337, 1078-1081, 2012.
- 22 Cohen, J., and Rind, D.: The effect of snow cover on the climate, *J. Climate*, 4, 689-
23 706, 1991.
- 24 Corbin, J. C., Pieber, S. M., Czech, H., Zanatta, M., Jakobi, G., Massabò, D., Orasche,
25 J., El Haddad, I., Mensah, A. A., and Stengel, B.: Brown and black carbon emitted
26 by a marine engine operated on heavy fuel oil and distillate fuels: optical
27 properties, size distributions, and emission factors, *J. Geophys. Res.-Atmos.*, 123,
28 6175-6195, 2018.
- 29 Dang, C., Brandt, R. E., and Warren, S. G.: Parameterizations for narrowband and
30 broadband albedo of pure snow and snow containing mineral dust and black
31 carbon, *J Geophys Res-Atmos*, 120, 5446-5468, 2015.
- 32 Dang, C., Fu, Q., and Warren, S. G.: Effect of Snow Grain Shape on Snow Albedo, *J.*
33 *Atmos. Sci.*, 73, 3573-3583, 2016.
- 34 Dang, C., Warren, S. G., Fu, Q., Doherty, S. J., and Sturm, M.: Measurements of light -
35 absorbing particles in snow across the Arctic, North America, and China: effects
36 on surface albedo, *J. Geophys. Res.-Atmos.*, 122, 10149-10168, 2017.
- 37 Ding, Q., Schweiger, A., L'Heureux, M., Steig, E. J., Battisti, D. S., Johnson, N. C.,
38 Blanchard-Wrigglesworth, E., Po-Chedley, S., Zhang, Q., and Harnos, K.:
39 Fingerprints of internal drivers of Arctic sea ice loss in observations and model
40 simulations, *Nat. Geosci.*, 12, 28-33, 2019.
- 41 Doherty, S. J., Warren, S. G., Grenfell, T. C., Clarke, A. D., and Brandt, R. E.: Light-

1 absorbing impurities in Arctic snow, *Atmos. Chem. Phys.*, 10, 11647-11680, 2010.
2 Doherty, S. J., Dang, C., Hegg, D. A., Zhang, R., and Warren, S. G.: Black carbon and
3 other light-absorbing particles in snow of central North America, *J. Geophys.*
4 *Res.-Atmos.*, 119, 12807-12831, 2014.
5 Dong, Z., Kang, S., Qin, D., Shao, Y., Ulbrich, S., and Qin, X.: Variability in individual
6 particle structure and mixing states between the glacier–snowpack and atmosphere
7 in the northeastern Tibetan Plateau, *The Cryosphere*, 12, 3877-3890, 2018.
8 Flanner, M. G., Liu, X., Zhou, C., Penner, J. E., and Jiao, C.: Enhanced solar energy
9 absorption by internally-mixed black carbon in snow grains, *Atmos Chem Phys*,
10 12, 4699-4721, 2012.
11 Flanner, M. G., Zender, C. S., Randerson, J. T., and Rasch, P. J.: Present-day climate
12 forcing and response from black carbon in snow, *J. Geophys. Res.*, 112, D11, 2007.
13 Grannas, A. M., Jones, A. E., Dibb, J., Ammann, M., Anastasio, C., Beine, H. J., Bergin,
14 M., Bottenheim, J., Boxe, C. S., Carver, G., Chen, G., Crawford, J. H., Domine,
15 F., Frey, M. M., Guzman, M. I., Heard, D. E., Helmig, D., Hoffmann, M. R.,
16 Honrath, R. E., Huey, L. G., Hutterli, M., Jacobi, H. W., Klan, P., Lefer, B.,
17 McConnell, J., Plane, J., Sander, R., Savarino, J., Shepson, P. B., Simpson, W. R.,
18 Sodeau, J. R., von Glasow, R., Weller, R., Wolff, E. W., and Zhu, T.: An overview
19 of snow photochemistry: evidence, mechanisms and impacts, *Atmos Chem Phys*,
20 7, 4329-4373, 2007.
21 Hadley, O. L., and Kirchstetter, T. W.: Black-carbon reduction of snow albedo, *Nat.*
22 *Clim. Change*, 2, 437-440, 2012.
23 He, C. L., Takano, Y., Liou, K. N., Yang, P., Li, Q., Chen, F., He, C., Takano, Y., Liou,
24 K. N., and Yang, P.: Impact of Snow Grain Shape and Black Carbon-Snow
25 Internal Mixing on Snow Optical Properties: Parameterizations for Climate
26 Models, *J. Climate*, 30, 10019-10036, 2017.
27 He, C. L., Flanner, M. G., Chen, F., Barlage, M., Liou, K. N., Kang, S. C., Ming, J.,
28 and Qian, Y.: Black carbon-induced snow albedo reduction over the Tibetan
29 Plateau: uncertainties from snow grain shape and aerosol-snow mixing state based
30 on an updated SNICAR model, *Atmos Chem Phys*, 18, 11507-11527, 2018a.
31 He, C. L., Liou, K. N., and Takano, Y.: Resolving Size Distribution of Black Carbon
32 Internally Mixed With Snow: Impact on Snow Optical Properties and Albedo,
33 *Geophys. Res. Lett.*, 45, 2697-2705, 2018b.
34 He, C. L., Liou, K. N., Takano, Y., Yang, P., Qi, L., and Chen, F.: Impact of Grain
35 Shape and Multiple Black Carbon Internal Mixing on Snow Albedo:
36 Parameterization and Radiative Effect Analysis, *J Geophys Res-Atmos*, 123,
37 1253-1268, 2018c.
38 Jacobson, M. Z.: Strong radiative heating due to the mixing state of black carbon in
39 atmospheric aerosols, *Nature*, 409, 695-697, 2001.
40 Kahnert, M., Nousiainen, T., Lindqvist, H., and Ebert, M.: Optical properties of light
41 absorbing carbon aggregates mixed with sulfate: assessment of different model
42 geometries for climate forcing calculations, *Opt. Express*, 20, 10042-10058, 2012.

- 1 Kokhanovsky, A. A., and Zege, E. P.: Scattering optics of snow, *Appl Optics*, 43, 1589-
2 1602, 2004.
- 3 Lack, D. A., and Cappa, C. D.: Impact of brown and clear carbon on light absorption
4 enhancement, single scatter albedo and absorption wavelength dependence of
5 black carbon, *Atmos. Chem. Phys.*, 10, 4207-4220, 2010.
- 6 Lack, D. A., Langridge, J. M., Bahreini, R., Cappa, C. D., Middlebrook, A. M., and
7 Schwarz, J. P.: Brown carbon and internal mixing in biomass burning particles,
8 *PNAS*, 109, 14802-14807, 2012.
- 9 Li, X., Kang, S., He, X., Qu, B., Tripathee, L., Jing, Z., Paudyal, R., Li, Y., Zhang, Y.,
10 and Yan, F.: Light-absorbing impurities accelerate glacier melt in the Central
11 Tibetan Plateau, *Sci. Total Environ.*, 587, 482-490, 2017.
- 12 Li, X., Kang, S., Zhang, G., Qu, B., Tripathee, L., Paudyal, R., Jing, Z., Zhang, Y., Yan,
13 F., and Li, G.: Light-absorbing impurities in a southern Tibetan Plateau glacier:
14 Variations and potential impact on snow albedo and radiative forcing, *Atmos. Res.*,
15 200, 77-87, 2018.
- 16 Liu, D. T., Whitehead, J., Alfarra, M. R., Reyes-Villegas, E., Spracklen, D. V.,
17 Reddington, C. L., Kong, S. F., Williams, P. I., Ting, Y. C., Haslett, S., Taylor, J.
18 W., Flynn, M. J., Morgan, W. T., McFiggans, G., Coe, H., and Allan, J. D.: Black-
19 carbon absorption enhancement in the atmosphere determined by particle mixing
20 state, *Nat. Geosci.*, 10, 184-U132, 2017.
- 21 Liu, J., Wu, D., Liu, G., Mao, R., Chen, S., Ji, M., Fu, P., Sun, Y., Pan, X., and Jin, H.:
22 Impact of Arctic amplification on declining spring dust events in East Asia, *Clim.*
23 *Dyn.*, 54, 1913-1935, 2020.
- 24 Liou, K. N., Takano, Y., and Yang, P.: Light absorption and scattering by aggregates:
25 Application to black carbon and snow grains, *J Quant Spectrosc Ra*, 112, 1581-
26 1594, 2011.
- 27 Liou, K. N., Takano, Y., He, C., Yang, P., Leung, L. R., Gu, Y., and Lee, W. L.:
28 Stochastic parameterization for light absorption by internally mixed BC/dust in
29 snow grains for application to climate models, *J Geophys Res-Atmos*, 119, 7616-
30 7632, 2014.
- 31 Liu, X., Zhou, C., Penner, J. E., and Jiao, C.: Enhanced solar energy absorption by
32 internally-mixed black carbon in snow grains, *Atmos. Chem. Phys.*, 12, 4699-
33 4721, <https://doi.org/10.5194/acp-12-4699-2012>, 2012.
- 34 Matsui, H., Hamilton, D. S., and Mahowald, N. M.: Black carbon radiative effects
35 highly sensitive to emitted particle size when resolving mixing-state diversity, *Nat.*
36 *Commun.*, 9, 1-11, 2018.
- 37 Meier, W. N., Hovelsrud, G. K., Van Oort, B. E., Key, J. R., Kovacs, K. M., Michel,
38 C., Haas, C., Granskog, M. A., Gerland, S., and Perovich, D. K.: Arctic sea ice in
39 transformation: A review of recent observed changes and impacts on biology and
40 human activity, *Rev. Geophys.*, 52, 185-217, 2014.
- 41 Moffet, R. C., and Prather, K. A.: In-situ measurements of the mixing state and optical
42 properties of soot with implications for radiative forcing estimates, *PNAS*, 106,

1 11872-11877, 2009.

2 Moteki, N., Kondo, Y., Miyazaki, Y., Takegawa, N., Komazaki, Y., Kurata, G., Shirai,
3 T., Blake, D. R., Miyakawa, T., and Koike, M.: Evolution of mixing state of black
4 carbon particles: Aircraft measurements over the western Pacific in March 2004,
5 *Geophys. Res. Lett.*, 34, L11803, 2007.

6 Peng, J. F., Hu, M., Guo, S., Du, Z. F., Zheng, J., Shang, D. J., Zamora, M. L., Zeng,
7 L. M., Shao, M., Wu, Y. S., Zheng, J., Wang, Y., Glen, C. R., Collins, D. R.,
8 Molina, M. J., and Zhang, R. Y.: Markedly enhanced absorption and direct
9 radiative forcing of black carbon under polluted urban environments, *PNAS*, 113,
10 4266-4271, 2016.

11 Pu, W., Wang, X., Wei, H., Zhou, Y., Shi, J., Hu, Z., Jin, H., and Chen, Q.: Properties
12 of black carbon and other insoluble light-absorbing particles in seasonal snow of
13 northwestern China, *The Cryosphere*, 11, 1213-1233, 2017.

14 Pu, W., Cui, J. C., Shi, T. L., Zhang, X. L., He, C. L., and Wang, X.: The remote sensing
15 of radiative forcing by light-absorbing particles (LAPs) in seasonal snow over
16 northeastern China, *Atmos. Chem. Phys.*, 19, 9949-9968, 2019.

17 Qian, Y., Gustafson, W. I., Leung, L. R., and Ghan, S. J.: Effects of soot-induced snow
18 albedo change on snowpack and hydrological cycle in western United States based
19 on Weather Research and Forecasting chemistry and regional climate simulations,
20 *J. Geophys. Res.-Atmos.*, 114, D3, 2009.

21 Ramanathan, V., and Carmichael, G.: Global and regional climate changes due to black
22 carbon, *Nat. Geosci.*, 1, 221-227, 2008.

23 Ricchiazzi, P., Yang, S., Gautier, C., and Sowle, D.: SBDART: A research and teaching
24 software tool for plane-parallel radiative transfer in the Earth's atmosphere, *Bull.*
25 *Amer. Meteor. Soc.*, 79, 2101-2114, 1998.

26 Schwarz, J. P., Gao, R. S., Perring, A. E., Spackman, J. R., and Fahey, D. W.: Black
27 carbon aerosol size in snow, *Sci. Rep.*, 3, 1356, 2013.

28 Shi, T., Pu, W., Zhou, Y., Cui, J., Zhang, D., and Wang, X.: Albedo of Black Carbon-
29 Contaminated Snow Across Northwestern China and the Validation With Model
30 Simulation, *J. Geophys. Res.-Atmos.*, 125, e2019JD032065, 2020.

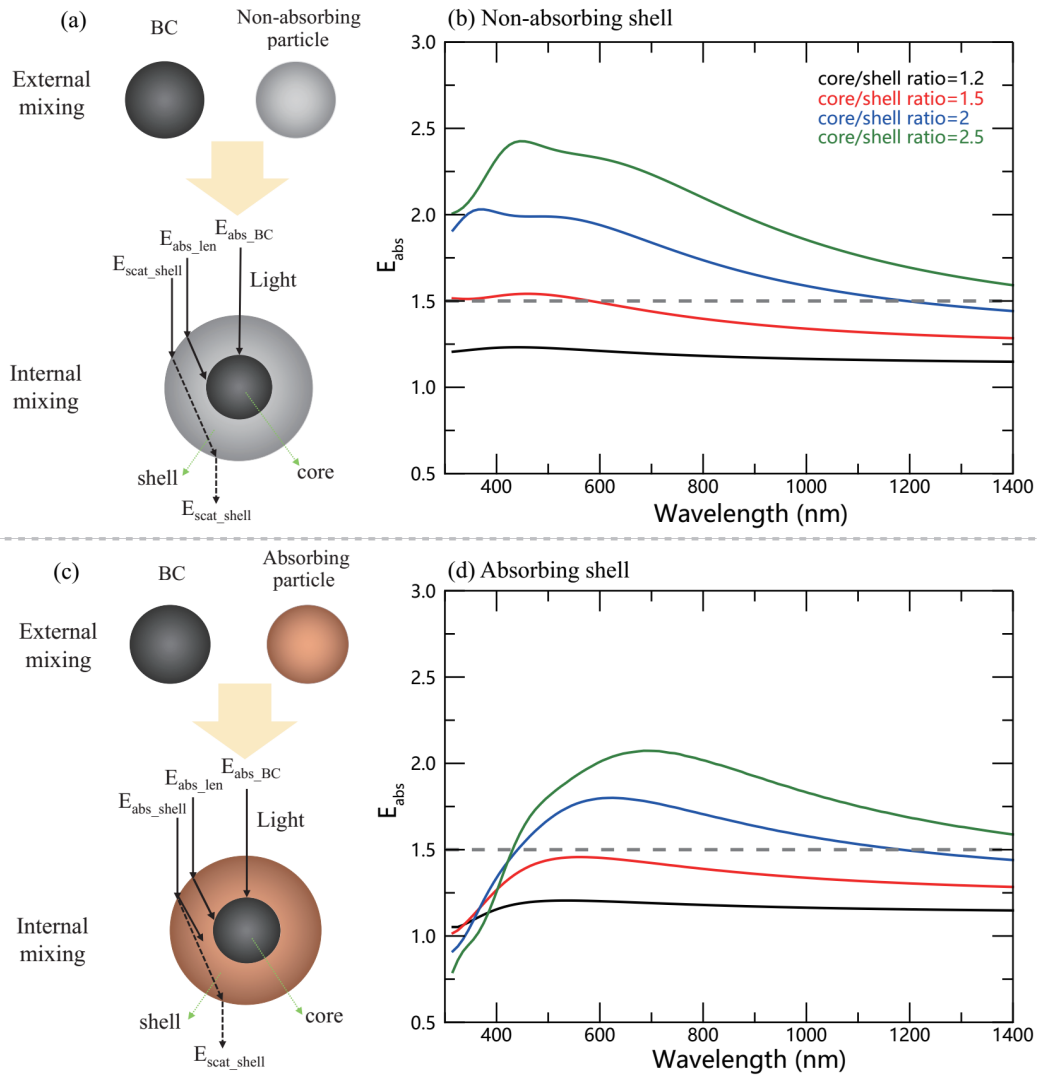
31 Sun, H. L., Biedermann, L., and Bond, T. C.: Color of brown carbon: A model for
32 ultraviolet and visible light absorption by organic carbon aerosol, *Geophys. Res.*
33 *Lett.*, 34, L17813, 2007.

34 Toon, O. B., McKay, C. P., Ackerman, T. P., and Santhanam, K.: Rapid Calculation of
35 Radiative Heating Rates and Photodissociation Rates in Inhomogeneous Multiple-
36 Scattering Atmospheres, *J. Geophys. Res.-Atmos.*, 94, 16287-16301, 1989.

37 Turpin, B. J., and Lim, H. J.: Species contributions to PM_{2.5} mass concentrations:
38 Revisiting common assumptions for estimating organic mass, *Aerosol Sci. Tech.*,
39 35, 602-610, 2001.

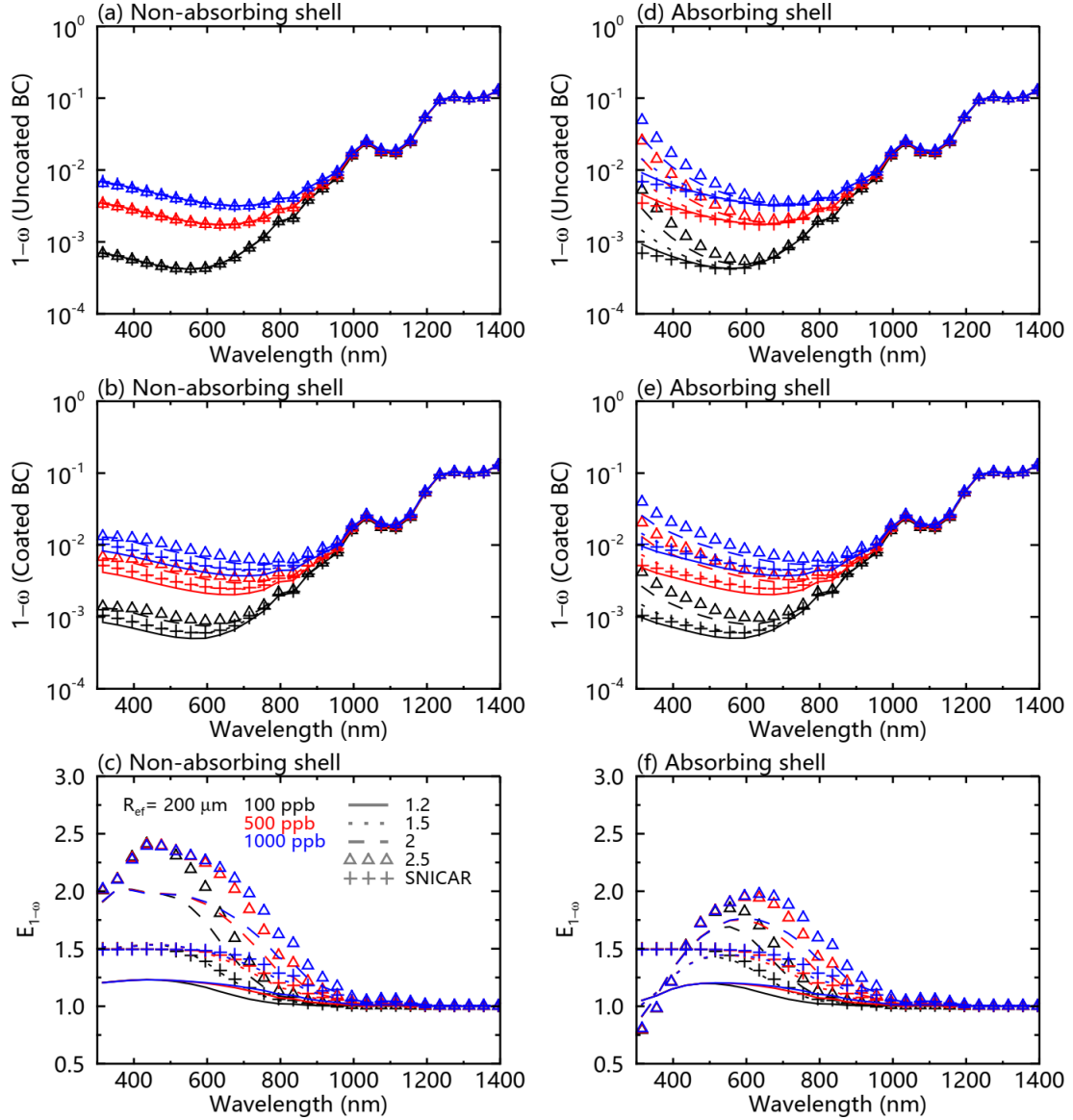
40 Wang, X., Doherty, S. J., and Huang, J.: Black carbon and other light-absorbing
41 impurities in snow across Northern China, *J. Geophys. Res.-Atmos.*, 118, 1471-
42 1492, 2013.

- 1 Wang, X., Pu, W., Ren, Y., Zhang, X. L., Zhang, X. Y., Shi, J. S., Jin, H. C., Dai, M.
2 K., and Chen, Q. L.: Observations and model simulations of snow albedo
3 reduction in seasonal snow due to insoluble light-absorbing particles during 2014
4 Chinese survey, *Atmos. Chem. Phys.*, 17, 2279-2296, 2017.
- 5 Warren, S. G., and Wiscombe, W. J.: A Model for the Spectral Albedo of Snow. 2:
6 Snow Containing Atmospheric Aerosols, *J. Atmos. Sci.*, 37, 2734-2745, 1980.
- 7 Xu, B. Q., Cao, J. J., Hansen, J., Yao, T. D., Joswila, D. R., Wang, N. L., Wu, G. J.,
8 Wang, M., Zhao, H. B., Yang, W., Liu, X. Q., and He, J. Q.: Black soot and the
9 survival of Tibetan glaciers, *PNAS*, 106, 22114-22118, 2009.
- 10 Yang, M., Howell, S. G., Zhuang, J., and Huebert, B. J.: Attribution of aerosol light
11 absorption to black carbon, brown carbon, and dust in China - interpretations of
12 atmospheric measurements during EAST-AIRE, *Atmos Chem Phys*, 9, 2035-2050,
13 2009.
- 14 Yao, T. D., Thompson, L., Yang, W., Yu, W. S., Gao, Y., Guo, X. J., Yang, X. X.,
15 Duan, K. Q., Zhao, H. B., Xu, B. Q., Pu, J. C., Lu, A. X., Xiang, Y., Kattel, D. B.,
16 and Joswiak, D.: Different glacier status with atmospheric circulations in Tibetan
17 Plateau and surroundings, *Nat. Clim. Change*, 2, 663-667, 2012.
- 18 Ye, H., Zhang, R., Shi, J., Huang, J., Warren, S. G., and Fu, Q.: Black carbon in seasonal
19 snow across northern Xinjiang in northwestern China, *Environ. Res. Lett.*, 7,
20 044002, 2012.
- 21 You, R., Radney, J. G., Zachariah, M. R., and Zangmeister, C. D.: Measured
22 Wavelength-Dependent Absorption Enhancement of Internally Mixed Black
23 Carbon with Absorbing and Nonabsorbing Materials, *Environ. Sci. Technol.*, 50,
24 7982-7990, 2016.
- 25 Zhang, Y., Kang, S., Cong, Z., Schmale, J., Sprenger, M., Li, C., Yang, W., Gao, T.,
26 Sillanpää, M., and Li, X.: Light - absorbing impurities enhance glacier albedo
27 reduction in the southeastern Tibetan Plateau, *J. Geophys. Res.-Atmos.*, 122,
28 6915-6933, 2017.
- 29 Zhang, Y., Kang, S., Sprenger, M., Cong, Z., Gao, T., Li, C., Tao, S., Li, X., Zhong, X.,
30 and Xu, M.: Black carbon and mineral dust in snow cover on the Tibetan Plateau,
31 *The Cryosphere*, 12, 413-431, 2018.



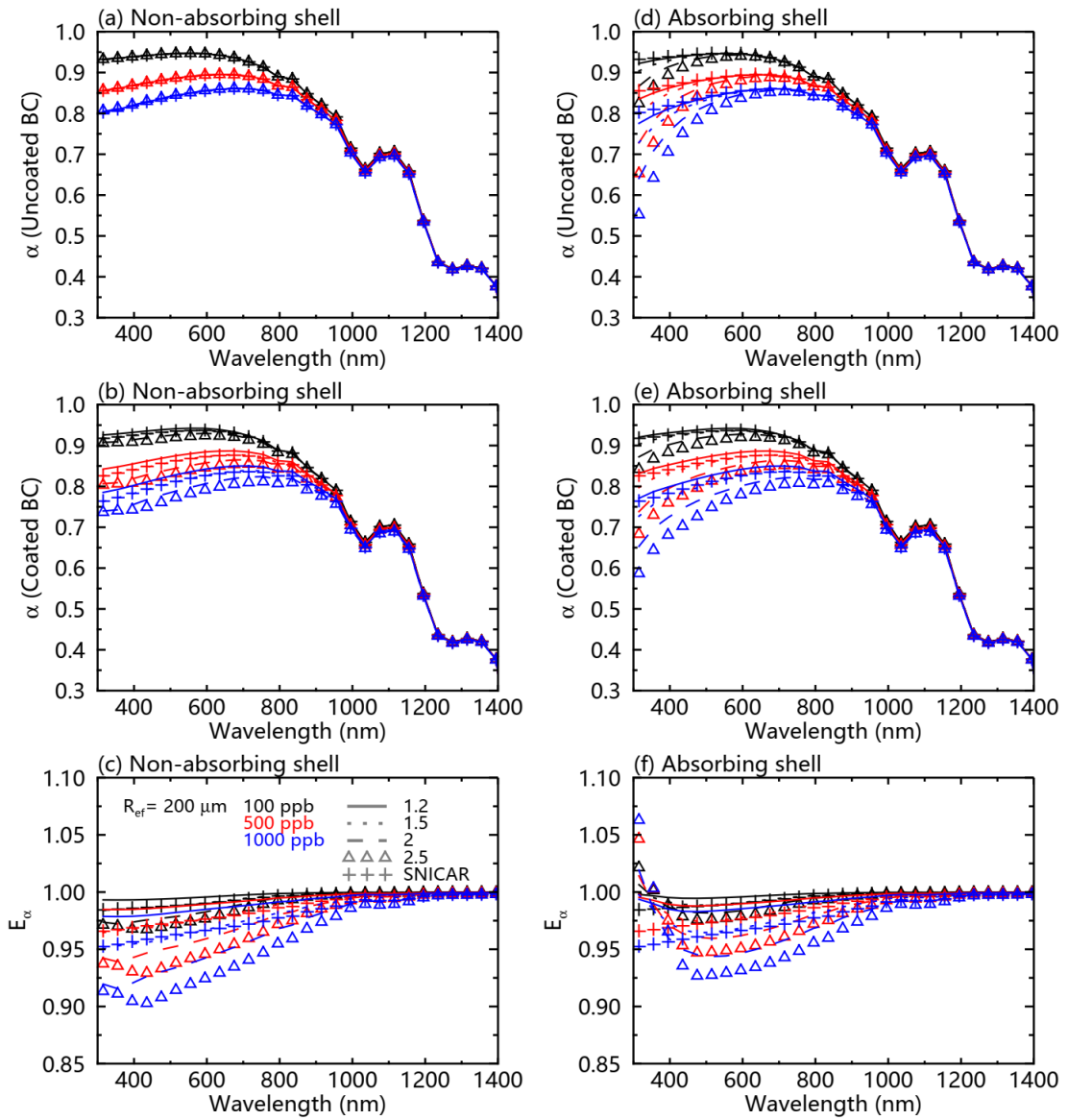
1
2
3
4
5
6
7
8

Figure 1. Schematic diagrams showing the light absorption for an external mixture and internal mixture of BC, for (a) a non-absorbing particle and (c) an absorbing particle. Also shown is the enhancement of light absorption from the internal mixture (E_{abs}) compared to the external mixture of BC with (b) non-absorbing and (d) absorbing particles. The internal mixed particle was assumed to be a core/shell structure with a black carbon (BC) core.



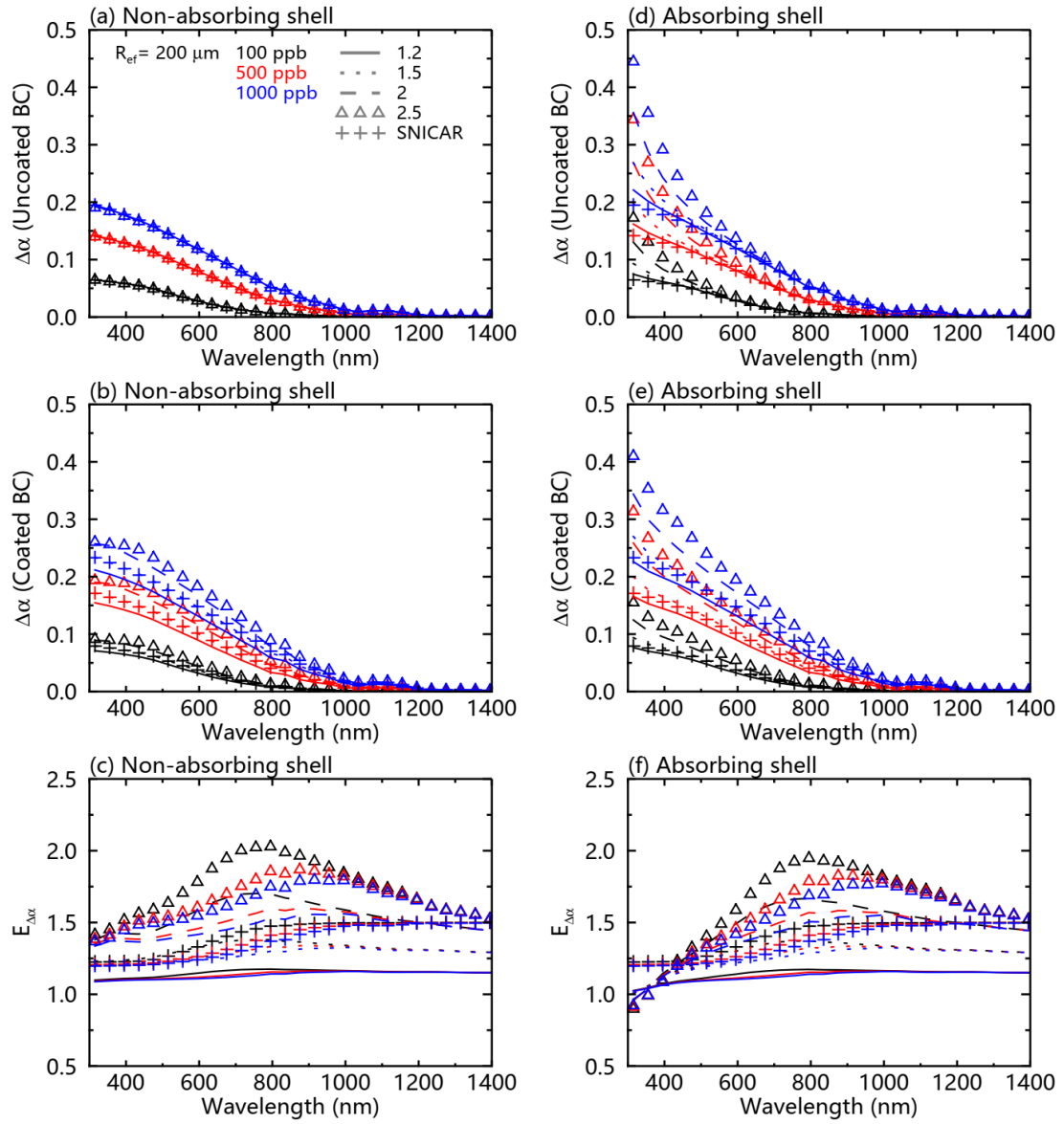
1
 2 **Figure 2.** Snow single-scattering co-albedo ($1-\omega$) as a function of wavelength, with
 3 different BC concentrations and core/shell ratios for (a) uncoated and (b) coated BC
 4 with an assumption of a non-absorbing shell. (d) and (e) are same as (a) and (b),
 5 respectively, but with an assumption of an absorbing shell. (c) shows the ratios of snow
 6 single-scattering co-albedo ($E_{1-\omega}$) for coated versus uncoated BC with an assumption
 7 of a non-absorbing shell. (f) is same as (c), but with an assumption of an absorbing shell.
 8 The snow grain radius was assumed to be 200 nm.

9
 10
 11
 12
 13



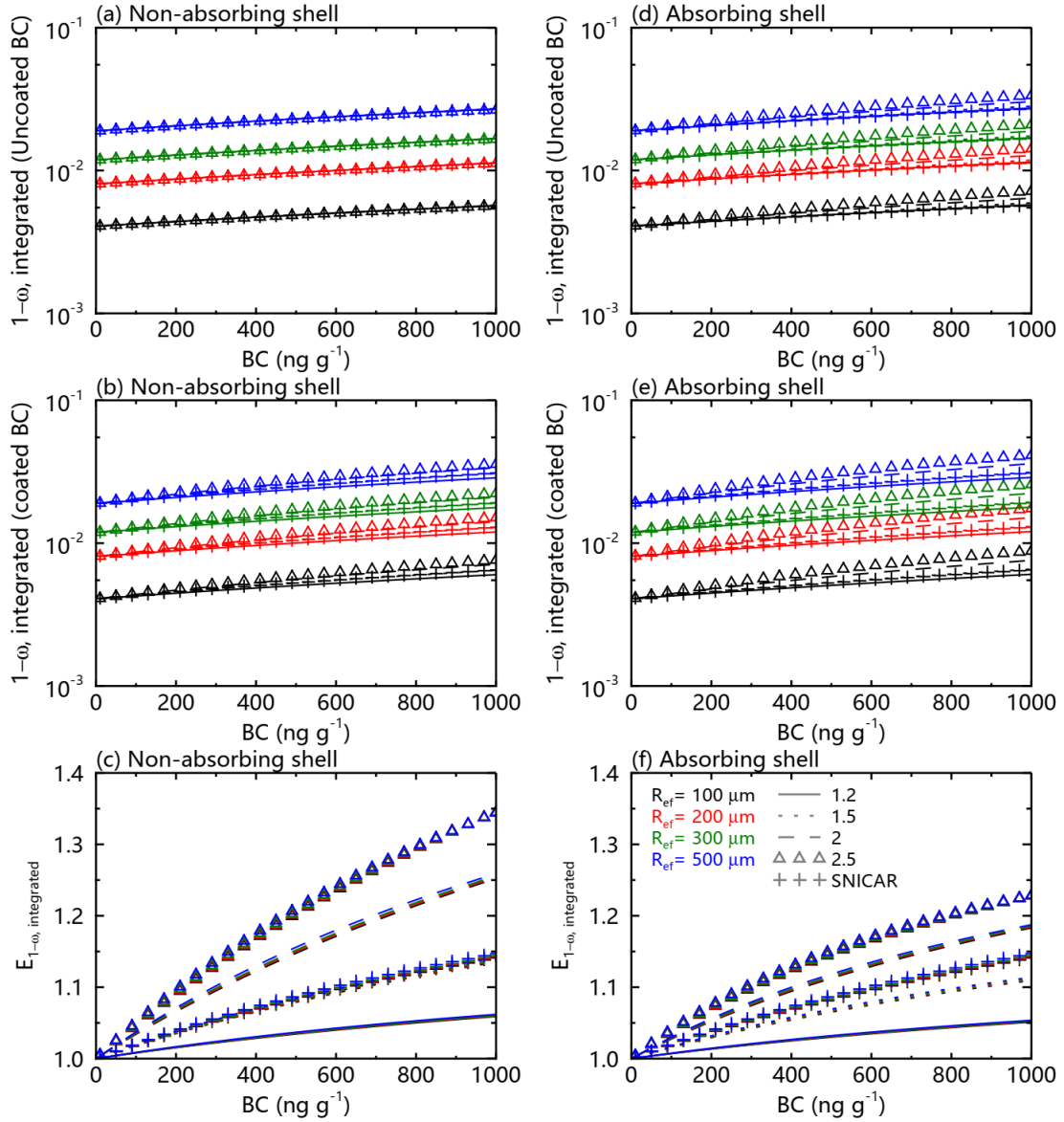
1
2
3

Figure 3. Same as Figure 2, but for snow albedo (α).



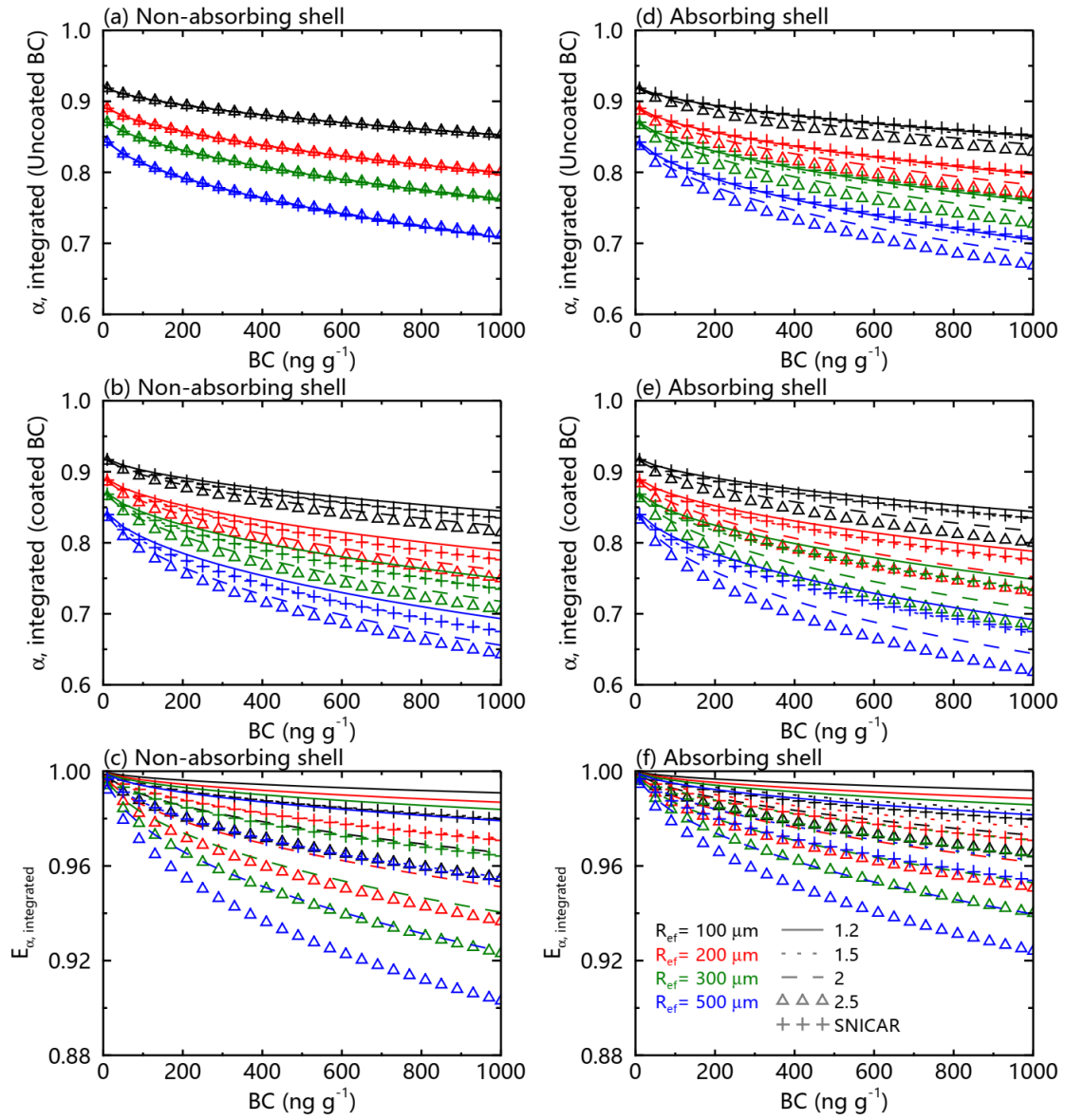
1
2
3

Figure 4. Same as Figure 2, but for snow albedo reduction ($\Delta\alpha$).



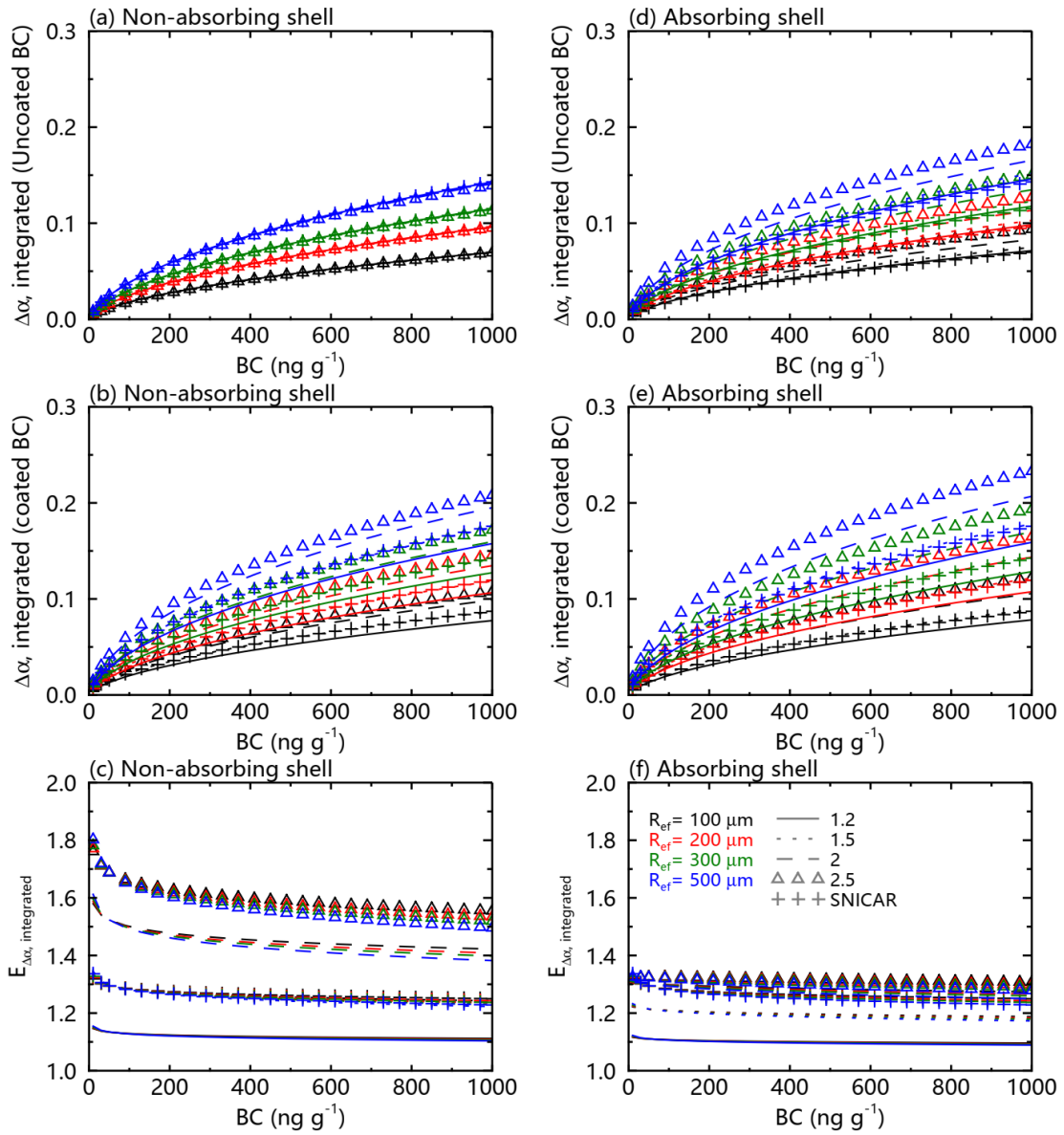
1
2
3
4
5
6
7
8
9

Figure 5. The spectrally weighted snow single-scattering co-albedo ($1-\omega_{\text{integrated}}$) over 300–2500 nm of a typical surface solar spectrum at mid–high latitude from January to May, for (a) uncoated and (b) coated BC with an assumption of a non-absorbing shell. (d) and (e) are same as (a) and (b), respectively, but with an assumption of an absorbing shell. (c) shows the ratios ($E_{1-\omega, \text{integrated}}$) of spectrally weighted snow single-scattering co-albedo for coated versus uncoated BC with an assumption of a non-absorbing shell. (f) is same as (c), but with an assumption of an absorbing shell.



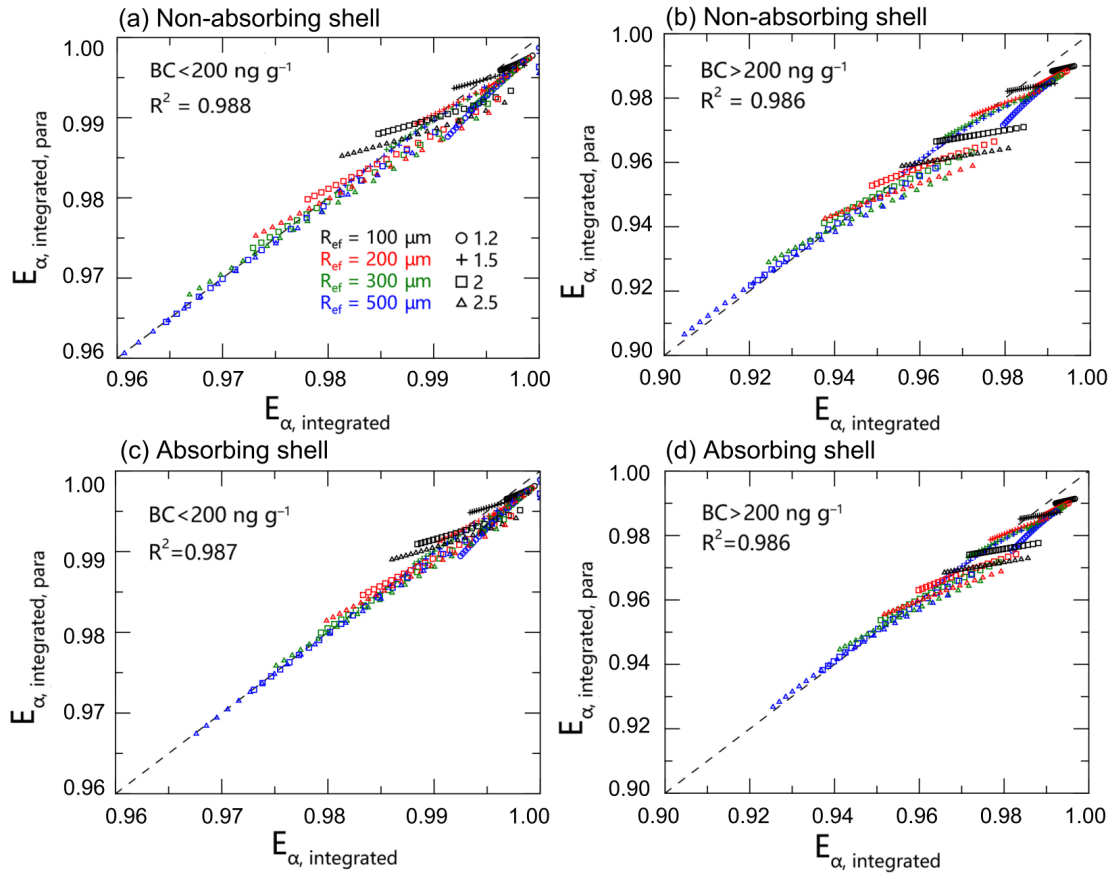
1
2
3

Figure 6. Same as Figure 5, but for snow albedo ($\alpha_{\text{integrated}}$).



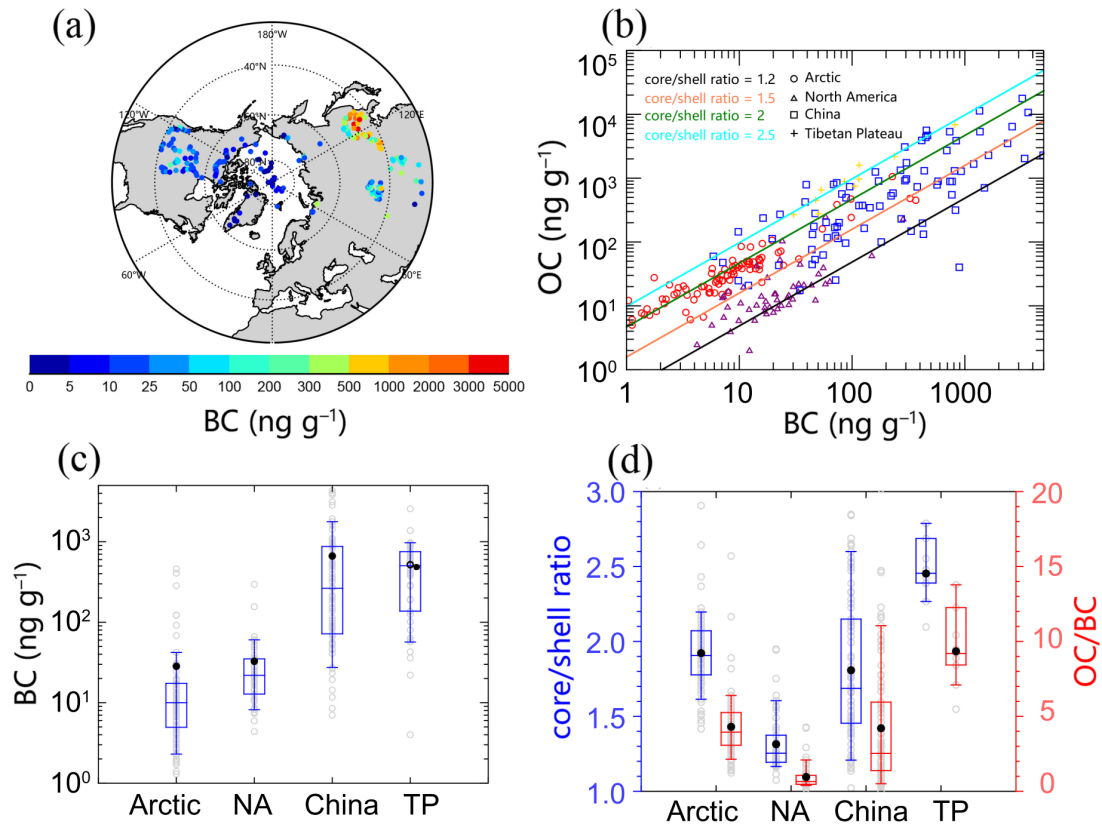
1
2
3

Figure 7. Same as Figure 5, but for snow albedo reduction ($\Delta\alpha_{\text{integrated}}$).



1
2
3
4
5
6

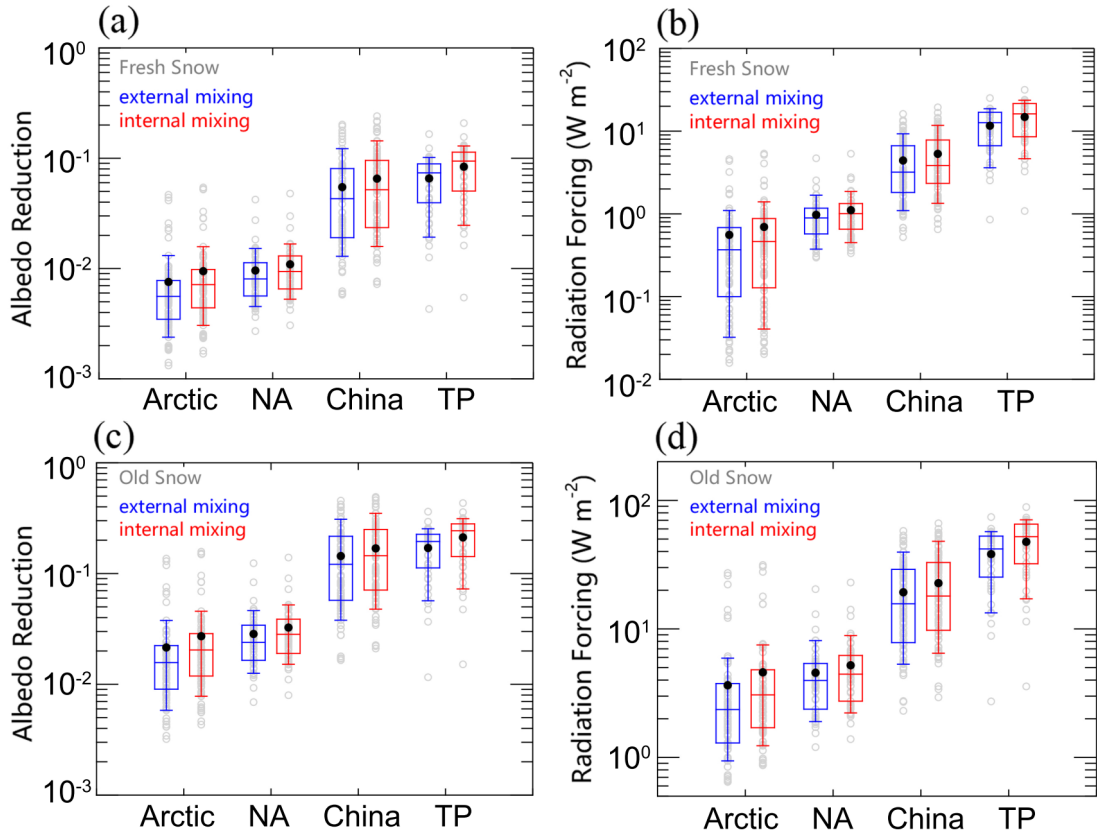
Figure 8. Comparisons of model calculated $E_{\alpha, \text{integrated}}$ and parameterized $E_{\alpha, \text{integrated, para}}$ for (a) relatively clean snow (BC concentration <200 ng g⁻¹), and (b) relatively polluted snow (BC concentration >200 ng g⁻¹) for a non-absorbing shell. (c) and (d) Same as (a) and (b), but for an absorbing shell.



1

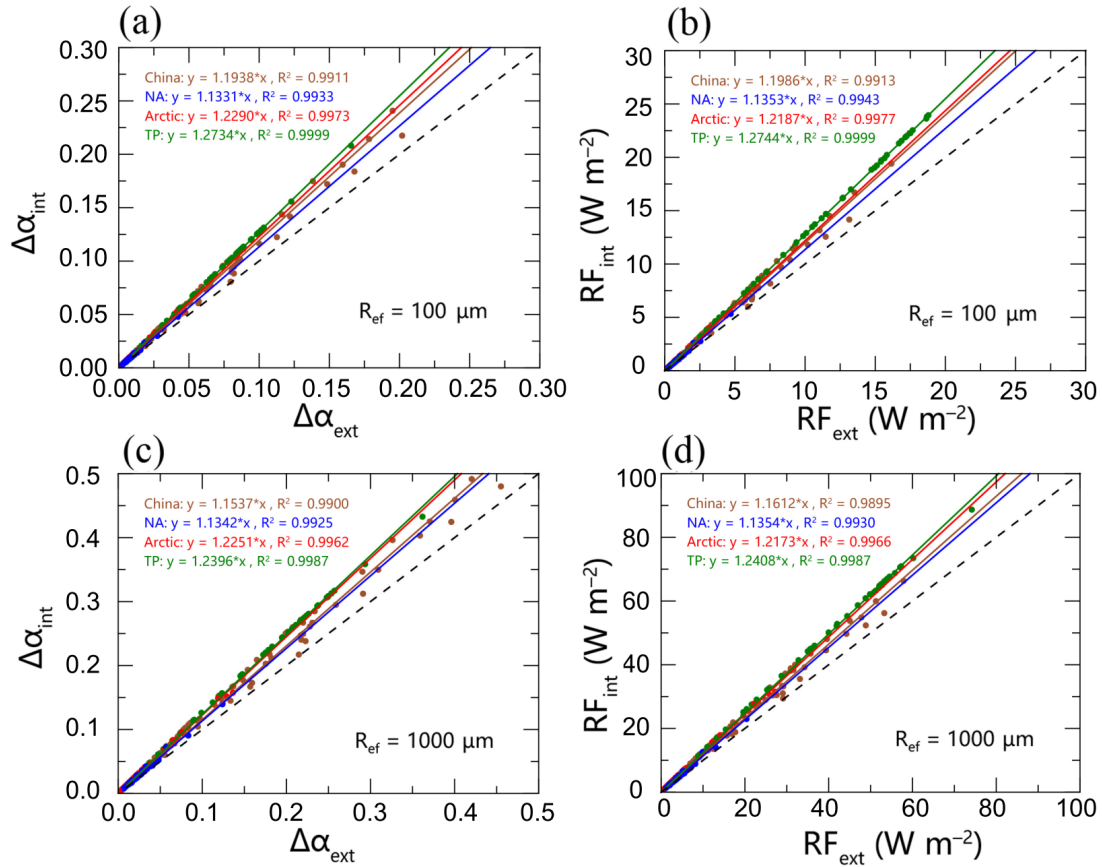
2 **Figure 9.** (a) The spatial distribution of measured black carbon (BC) concentrations
 3 across the Northern Hemisphere. (b) Comparison of BC and organic carbon (OC)
 4 concentrations in: the Arctic, North America (NA), northern China (NC) and the
 5 Tibetan Plateau (TP). (c) Statistical plots of BC concentrations in different regions. The
 6 boxes denote the 25th and 75th quantiles, the horizontal lines denote the 50th quantiles
 7 (medians), solid dots denote averages, and whiskers denote the 10th and 90th quantiles.
 8 In situ data is shown as gray circles. (d) Same as (c) but for a core/shell ratio and OC/BC
 9 mass ratio, assuming a core/shell structure with a BC core and an absorbing OC shell.

10



1
 2 **Figure 10.** Statistical plots of (a) albedo reduction, and (b) radiative forcing, in different
 3 regions for fresh snow. (c) and (d) Same as (a) and (b), but for old snow. The boxes
 4 denote the 25th and 75th quantiles, horizontal lines denote the 50th quantiles (medians),
 5 solid dots denote averages, and whiskers denote the 10th and 90th quantiles. In situ data
 6 is shown as gray circles.

7



1

2 **Figure 11.** Comparisons of (a) the snow albedo reduction and (b) the radiative forcing
 3 by an internal mixed particle versus an external mixed particle, based on in situ
 4 measurements of fresh snow (assuming a snow grain radius of 100 μm). (c) and (d)
 5 Same as (a) and (b), but for old snow and assuming a snow grain radius of 1000 μm.